Regaining Control: Investigating the cause of knee hyperextension during stance phase in predictive simulation of running

MSc Thesis Biomedical Engineering

Floor Janssen (4655168) Delft University of Technology
Supervisors: Eline van der Kruk (TU Delft), Robert-Jan de Vos (Erasmus MC)

January 22, 2024

Abstract

Running is one of the most practiced sports worldwide, offering numerous health benefits, but also carrying a risk of injury, mainly at the knee and ankle joints. The origin of running injuries is not fully understood. With predictive neuromusculoskeletal simulations, more insight could be gained into the biomechanical mechanisms that may lead to injuries. However, in predictive simulations of gait, hyperextension of the knee during stance phase is often encountered. This limits their applicability in research into running-related injuries. It is unclear what causes these unrealistic kinematics, with various studies coming to conflicting conclusions. This study aims to identify the cause of knee hyperextension in predictive models of running and subsequently, to determine the essential modeling elements for accurately simulating stance knee flexion.

A structured analysis was conducted to investigate the potential impact of the model components within the predictive simulation framework. This framework was divided into four main categories: the objective function, the musculoskeletal (MSK) model, the foot contact model, and the controller. The analysis resulted in numerous hypotheses regarding the element that might be responsible for the simulation of realistic knee kinematics. SCONE, an open-source package for neuromusculoskeletal predictive simulation, was used to test the effect of each hypothesis on the simulated running kinematics. The simulation outcomes were compared to experimental data to assess possible improvements.

The results demonstrate that, in contrast to previous literature, adaptations to the objective function, the MSK model, and the foot contact model have negligible effects on predicted running kinematics. This leads to the conclusion that the controller is essential to focus on when improving knee kinematics. Due to time constraints, multiphase control could not be implemented. Therefore, the exact reflex pathways and phase transitions should be further investigated for the predictive simulation of running before implementation is possible.

1 Introduction

Running is one of the most practiced sports in the Netherlands and worldwide.[1][2][3][4] Running is associated with a decreased risk of obesity, depression, and type II diabetes[5][6][7]. However, it is also associated with high injury rates, preventing people from fully enjoying these health benefits and leading to increased healthcare costs.[8] Running-related injuries most frequently occur around the knee and ankle.[9] Depending on the exact injury, these might be caused by extrinsic risk factors like the stiffness of the running surface[10][11], footwear[11][12][13][14][15], and running style[14][16][17][18] and experience[11][17][19][20], but also by intrinsic risk factors like hindfoot alignment[21][22][23], longitudinal foot arch[11][19][22], muscle strength[19][24] and tissue structure[25][26][27].

Many of these risk factors are not definitive, with studies providing limited, or even conflicting evidence, such as the influence of the longitudinal foot arch or the hindfoot alignment. A better understanding of the injury mechanisms of knee and ankle running injuries could be gained by studying biomechanical measures such as mechanical joint loading and loading rate[28][29], breaking force[30] and tendon stress

patterns[27]. With human research, most of these measures can only be measured using invasive methods, if at all. On the other hand, with predictive neuromusculoskeletal modeling direct analysis of the previously listed biomechanical measures is possible. The effects of, for example, an increase in muscle strength or surface stiffness on the knee and ankle joint loads can be implemented and studied directly when making use of predictive simulation. However, to accurately simulate these effects and gain insight into the origin of injuries, the simulation of realistic knee and ankle kinematics is essential.

Predictive neuromusculoskeletal simulations can generate motion *de novo*. This process is called predictive simulation (Figure 1). The predictive simulation framework consists of multiple parts. First, a musculoskeletal model that models the joints, muscles, and segment properties. Second, a contact model that models the interaction between the feet and the environment. Third, a controller that controls the muscle activations, imitating neural control and thus controls the actuation of the musculoskeletal model. Fourth, an objective function that solves the redundancy problem and specifies the goal of the motion, and lastly, an optimization algorithm that searches the optimal controller parameters by minimizing the objective function. The optimization algorithm searches for the control parameters that result in the best fitness value for the given objective function. An initial guess of the control parameters can be used for the first simulation to reduce simulation times.

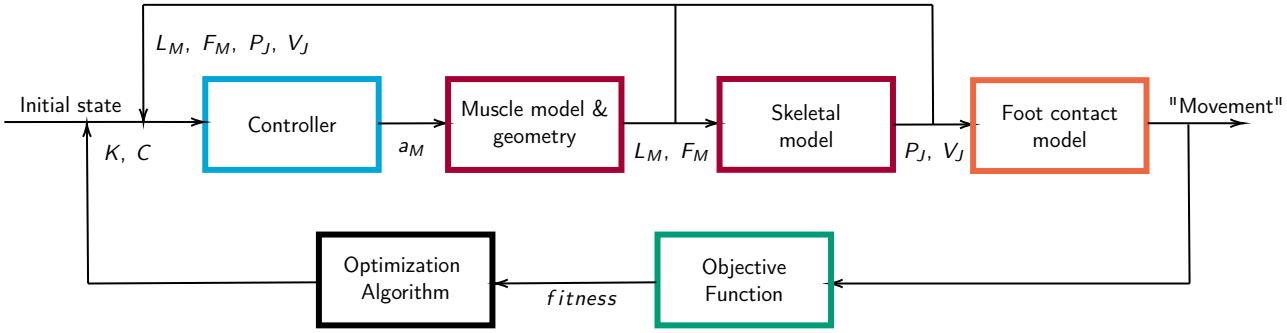

Figure 1: Predictive simulation framework for feedback-based optimization. K refers to the feedback gains, and C to the constants that are optimized.L_M,F_M,P_J,V_J refer to muscle length and force and joint position and velocity respectively. These are the parameters that might be optimized in a feedback-based controller. Not every model implements all components.

Over the past twenty years, predictive modeling of human gait has progressed from rigid body models that took hours to solve, to multidimensional, more realistic, and biologically accurate models that can be solved and optimized in less than an hour.[31] Rigid body models have resulted in a better understanding of the biomechanics and control mechanisms in gait[32][33][34][35][36], but are limited in their use in practical and clinical settings. The recent advancement to more complex models, that include musculature and neural control, has freed the way to more applied research, like studying the effect of orthosis designs or muscle weakness on the predicted walking pattern.[37][38]

In the predictive simulation of human movement, two main groups of controllers can be used: open-loop algorithms and neural feedback (or closed-loop) controllers.[39] Open-loop controllers are generally faster but do not include sensory feedback and are therefore limited in their applicability for studies focusing on control and compensatory strategies. Neural control, on the other hand, includes sensory feedback, making it more useful for studying adaptation strategies.[39] Three types of neural controllers exist: P, PD, and reflex controllers. The last group behaves like extended P controllers, using proportional control for muscle reflexes and PD control for vestibular reflexes.[40] Reflex control is the primarily used control method in studies focusing on the predictive simulation of gait.[40]

A neural reflex controller simulates the muscle reflexes of the neural system that controls the muscle activations. Reflex pathways can be split up into vestibular reflexes, which act based on the position of predefined joints, and muscle reflexes, which react based on the muscle's length and/or force. These reflexes can be monosynaptic or antagonistic. In essence, a reflex controller models the reflex loops from the muscle spindles (length) and the Golgi tendon organs (force) to the central nervous system and back to the muscle. The degree of trust in the information from each sensory system is modulated in humans.[41] This modulation is captured in a predictive model by reflex gains. These are optimized in the

optimization algorithm. The pathways that are present in a controller can be pre-specified for separate phases in the gait cycle. For each phase, different feedback gain magnitudes are determined. Which feedback pathway and phases are present differs per model.

Previous musculoskeletal predictive simulations of gait have mostly focused on walking, with a few exceptions that have studied the predictive simulation of running, with none yet published that used neural control.[35][42][43] The distinction between walking and running is made based on the presence of a double support phase in walking, where both limbs touch the ground, and the presence of a flight phase in running, during which both limbs are off the ground.[44] In most people, the transition from walking to running happens based on forward speed, with running being more efficient and stable for higher speeds and thus preferred for those speeds.[45] However, the preferred transitioning speed is not the same in each individual, and can also be overruled in for example race-walking, which makes speed unsuitable to make the distinction between walking and running. Comparing the biomechanics of running and walking reveals similar muscle activation patterns, distinguished by earlier activation of the ankle plantar flexors and quadriceps muscle during stance in running.[46] Nevertheless, similar lower limb kinematic patterns are observed in both walking and running, with both showing a distinctive peak in knee flexion with subsequent knee extension during both swing and stance. Additionally, both walking and running show peak in ankle dorsiflexion, followed by a peak in plantarflexion. Due to the limited availability of studies focusing on the predictive simulation of running and the kinematic similarities between walking and running, both are considered in this study.

Modeling choices can severely impact the resulting knee and ankle kinematics. Falisse et al. [39] failed to simulate realistic knee and ankle kinematics in combination with realistic kinetics in both walking and running while using a three-dimensional model with open-loop trajectory optimization. In Ong et al. [38], their two-dimensional reflex-based model lacked distinct knee flexion and subsequent extension during stance phase, instead showing knee hyperextension throughout the stance phase in the predictive simulation of walking. This problem was also observed in the predictive simulation of running, using an adapted version of a two-dimensional reflex-based model by Geijtenbeek [unpublished work].

On the other hand, numerous studies focusing on the predictive simulation of gait have achieved accurate knee and ankle stance phase kinematics with a range of different modeling choices. Falisse et al. [47] showed improved knee and ankle kinematics by adding a passive toe joint and decreasing the Achilles tendon stiffness in a three-dimensional open-loop model. Additionally, Waterval et al. [37] also showed improvement when a toe joint was added to the model used in Ong et al. [38] and Veerkamp et al. [48]. Notably, in Van der Kruk and Geijtenbeek [49], realistic walking kinematics were achieved in both knee and ankle during the stance phase without the presence of a toe joint, using a two-dimensional reflex-based model with additional lumbar and thoracic joints. In Veerkamp et al. [48] it was shown that the predicted walking kinematics in a two-dimensional reflex-based model are highly dependent on the terms involved in the objective function.

Collectively, different model and controller designs lead to differences in outcomes, with the simulation of realistic knee and ankle kinematics emerging as a significant challenge. The precise modeling elements contributing to the simulation of realistic knee and ankle kinematics remain unclear, with studies showing countering strategies that are not always universally applicable. This limits the practical application of these models in research on running-related injuries. Therefore, this study aims to determine the cause of knee hyperextension in the predictive modeling of running and subsequently, to find the essential modeling elements for accurately simulating stance knee flexion and subsequent ankle dorsiflexion during stance phase in running, within planar reflex-based predictive models. This was done by a systematic analysis of the potential influence of the components of the predictive simulation framework, focusing on planar reflex-based models. The components have been categorized into four domains: the objective function, the musculoskeletal (MSK) model, the foot contact model, and the controller. Hypotheses that have been proposed in previous studies were investigated, and new hypotheses were formed and tested using predictive simulations.

2 Hypotheses

Three sources were used to formulate hypotheses in each of the four domains of the predictive simulation framework that may explain stance knee hyperextension in the predictive simulation of running: previously proposed improvements, novel hypotheses, and a comparison between models that demonstrate realistic kinematics.

2.1 Previously proposed improvements

2.1.1 Musculoskeletal model

In a recent study by Falisse et al. [47], the effect of changes in the musculoskeletal model on the lower limb kinematics was investigated. Adding a toe joint to their three-dimensional model improved knee kinematics but worsened ankle kinematics. Additionally, the study found that decreasing the Achilles tendon (AT) stiffness by 60% improved ankle kinematics.[47] Falisse et al. [47] also found that altering the weight distribution to a lighter torso and heavier legs positively affected knee kinematics. However, this adaptation was shown to be less stable than the first two (toe joint and AT stiffness) and is therefore unlikely to be the main element responsible for the simulation of realistic knee and ankle kinematics. This led to the first set of hypotheses:

More realistic stance knee kinematics are achieved by:

H_MSK1 Adding a toe joint.

H_MSK2 Reducing the Achilles tendon stiffness by 60%.

2.1.2 Objective function

Multiple studies have focused on the effect of the objective function on the simulated kinematics in gait. An objective function can be split into two parts: a main objective that is minimized throughout the optimization and penalty terms that go to zero when certain requirements are met.

The main objective deals with the redundancy problem. There are multiple theories on how the body chooses which muscles to recruit. They can be mostly split up into two groups: cost-of-transport (CoT) objectives that minimize metabolic cost over distance, and activation-based objectives that minimize the muscle activation levels.[50]

Activation-based objectives generally result in better running kinematics than cost-of-transport-based objectives.[51] The overall most realistic walking kinematics and kinetics were achieved using a combination of an activation-based and a CoT term in the objective. However, while improved, the predicted knee mechanics remained inaccurate.[39] Veerkamp et al. [48] also found that a combined objective with both a CoT and a muscle activation term resulted in more realistic walking kinematics in 2D simulations of gait. Veerkamp et al. [48] found the most realistic kinematics when adding a minimizing head acceleration and a maximum ground reaction force penalty term in the objective. This leads to the following hypotheses that more realistic stance knee kinematics are achieved by:

H_O1 Minimizing muscle activations.

H_O2 Minimizing muscle activations and CoT.

H_O3 Minimizing head acceleration.

H_O4 Adding a maximum ground reaction force.

2.1.3 Foot contact model

Recent studies have suggested that the performance of a predictive simulation is highly dependent on the foot contact model.[47][52] In Falisse et al. [47], it was shown that a more superior vertical location of the contact spheres improved the knee kinematics, but resulted in worsened ankle kinematics. However, this was not a stable solution and is thus not considered further.[47] Furthermore, an ellipsoid foot showed more accurate kinematics when compared to a foot model with spherical contact elements at the heel and toes when both versions were simulated to track the measured center of pressure data.[52] However, when a free simulation was performed without previously measured data, the ellipsoid foot induced unrealistically high ground reaction forces while the spherical element foot resulted in realistic ground reaction forces and foot kinematics.[52] This leads to the conclusion that using spherical foot contact model elements is overall better for the simulation of gait.

2.2 Novel Hypotheses

2.2.1 Objective function and foot-contact model

Joint loads are defined as the sum of the resultant forces and moments acting between two articulating bones. These represent the forces that would otherwise act on the unmodelled soft tissue structures such as cartilage and ligaments.[53] High joint loads can cause pain and joint damage and are therefore prevented.[54] Although a computer-generated model cannot feel pain, a joint load penalty can be added to the objective function to simulate it. The work of the joints is said to play a pivotal role in the distribution of the impact forces.[55] In line with this, increased knee flexion, and ankle dorsiflexion could decrease joint loading, which is highest during stance. Therefore, a hypothesis was formed that a joint load penalty term could induce knee flexion and ankle dorsiflexion during stance phase.

More realistic stance knee kinematics are achieved by:

H_O5 Adding a joint load penalty for the hip, knee and ankle joints.

Observations in barefoot and shod runners support the notion that the body uses the foot and ankle joints for energy distribution. Habitual barefoot runners tend to exhibit more forefoot running compared to those wearing cushioned shoes.[56] With forefoot running, the ankle joint is used more effectively to store energy.[56] Therefore, is theorized that the more flexible shoes may assume the role of the foot and ankle in energy storage when compared to the barefoot, stiffer contact, scenario. In line with the theory behind H_O, a stiffer foot contact sphere would be expected to result in increased knee flexion.

More realistic stance knee kinematics are achieved by:

H_FC1 Increasing the stiffness of the foot contact spheres.

2.2.2 Controller

The concept of static stability is relatively simple: if the center of mass of a system is outside the triangle of support, the system is statically unstable. In the context of running, however, the center of mass is frequently located near the edge of the triangle of support or even beyond the edge, resulting in a statically unstable system. Therefore, an alternative definition for running stability is needed. Locomotor, or dynamic, stability is defined as the ability to return to a steady-state, periodic gait after a perturbation.[57] In humans, the vestibular system is used to estimate head acceleration, with its feedback gain increasing in more unstable situations.[58] This means that the input of the vestibular system is considered more important in unstable situations. In, Magnani et al. [58] a rise in vestibular feedback gain magnitude during early stance phase was measured. This coincides with the period of initial knee flexion during stance phase and indicates that early stance is an unstable moment in gait, which may be counteracted by knee flexion.

Furthermore, in D'Hondt et al. [59] the extension from 2D to 3D introduced knee flexion in stance phase.[59] A 3D model is inherently more unstable because it requires medial-lateral stability. The knee flexion might thus be a reaction to the more unstable situation. This leads to the following hypothesis:

More realistic stance knee kinematics are achieved by:

H_C1 An increased need for stability.

2.3 Model Comparison

The final source of hypotheses compared two models with, and without realistic stance phase kinematics. The realistic gait model that was used was H1120_WALK from Van der Kruk and Geijtenbeek [49]. This model was compared to a simple running model, adapted from Geijtenbeek [unpublished work], H0920_RUN, which showed stance knee hyperextension. The differences between these models possibly account for the relative presence/absence of knee flexion during the stance phase. A schematic overview of both models is shown in Figure 2.

2.3.1 Musculoskeletal model

There are three main differences between H0920 and H1120. Firstly, the presence of a torque-driven thoracic and lumbar joint in H1120. Secondly, in H0920 the muscle parameters were based on a combination of the OpenSim Gait2392 model by Delp et al. [60] and the updated ones proposed by Rajagopal et al. [61], while in H1120 the muscle parameters, tendon slack length, optimal length and pennation angle,

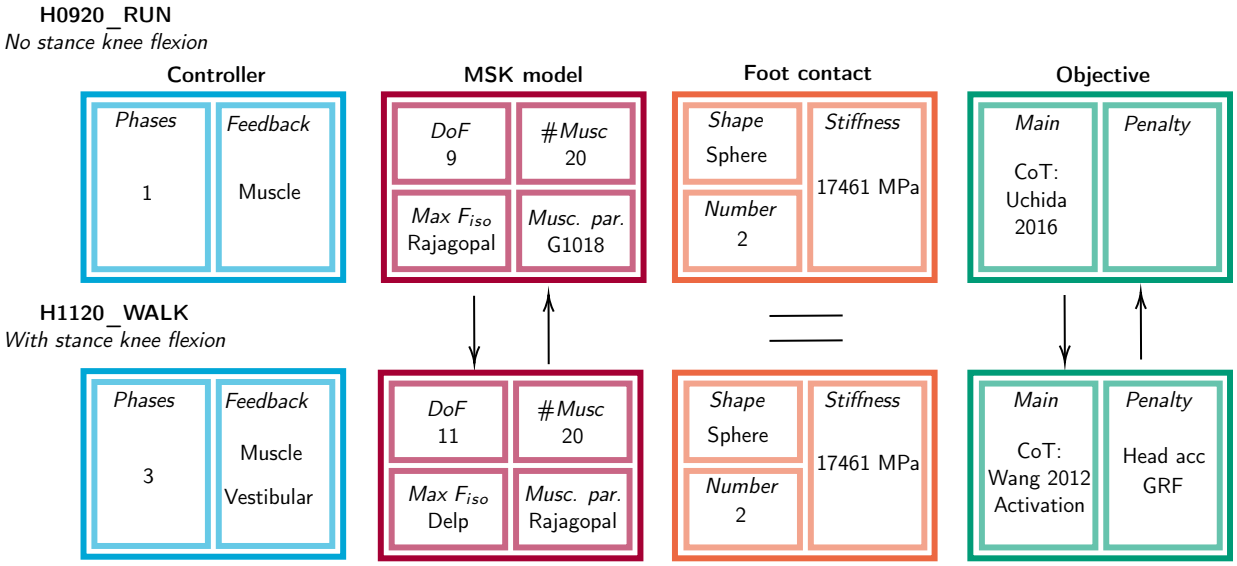

Figure 2: The main differences between a model showing realistic stance knee kinematics (H1120_WALK) and one that does not (H0920_RUN).

were based on Arnold et al. [62]. Lastly, in H0920 the maximum isometric muscle forces were based on the Opensim Gait2392 model.[60], while in H1120 these were based on Rajagopal et al. [61]. There was no difference between the respective foot contact models. This led to the following hypotheses:

More realistic stance knee kinematics are achieved by:

H_MSK3 Adding a lumbar and a thoracic joint

H_MSK4 Implementing the muscle parameters from the OpenSim Gait2392 model[60] and the updated ones proposed by Rajagopal et al. [61].

H_MSK5 Implementing the maximum isometric forces from the OpenSim Gait2392.[60]

2.3.2 Objective function

The objective function used in H1120_WALK is similar to the objective function proposed in Veerkamp et al. [48]. The differences between the objectives used in H1120_WALK and H0920_RUN will therefore be evaluated according to hypotheses H_O2, H_O3, and H_O4.

2.3.3 Controller

Both controllers in H0920_RUN and H1120_WALK are neural reflex controllers. A complete overview of the feedback pathways and optimization parameters is given in Appendix A. There are two main differences between both controller designs. First, H1120_WALK incorporates vestibular feedback of the position and velocity of the upper body. Second, the controller used in H1120_WALK distinguishes three separate phases in the gait cycle: stance, lift-off, and swing. In H0920_RUN no division in phases is present. It is hypothesized that more realistic stance knee kinematics are achieved by:

H_C2 Adding a vestibular feedback pathway.

H_C3 Adding multiple phases to the controller.

3 Methods

To test the hypotheses, new predictive simulations were run, based on an adapted version of a simple running model by Geijtenbeek [unpublished work]: H0920_RUN. The simulations were run in SCONE: an open-source software package for predictive neuromusculoskeletal modeling.[63] The kinematic outcomes of each simulation were compared to kinematic experimental data from Hamner et al. [64]. Improvement of the knee kinematics was defined as knee flexion, and subsequent extension during stance phase, creating a clear peak in knee flexion during stance phase, separate from the peak seen during swing phase. A full overview of all muscle activations, joint loads, and joint moments for all simulated scenarios can be found in Appendix E.

3.1 Simulation framework

This study's simulations were conducted in SCONE, an open-source software package for predictive neuromusculoskeletal modeling.[63] The optimizations were performed using the covariance matrix adaptation evolutionary strategy (CMA-ES) algorithm by Hansen [65] until the fitness had not improved by more than 0.01% per generation over the last 500 generations.

The duration of the simulations was set to 15 seconds to make sure a stable gait cycle was reached. For each scenario, five parallel optimizations were executed, each with a slightly different initial state. The optimization with the best (minimum) fitness score was used in the further analysis.

The outcome of each simulation was averaged over the complete gait cycles measured within one simulation. Outcomes were compared to the averaged experimental data. Gait cycles were normalized from 0 to 100% where 0% corresponds with foot strike and 100% with the next foot strike of the same foot. Stance phase was defined as foot-strike to toe-off and identified as the duration of which the magnitude of the ground reaction forces was above 8 N. This threshold was chosen to remove inconsistencies in the data. Gait cycles were taken out if they were shorter than 85% of the average duration of all gait cycles within that simulation to remove incomplete gait cycles.

All simulations were based on H0920_RUN, adaptations were made to test each hypothesis.

3.2 H0920_RUN

Musculoskeletal model

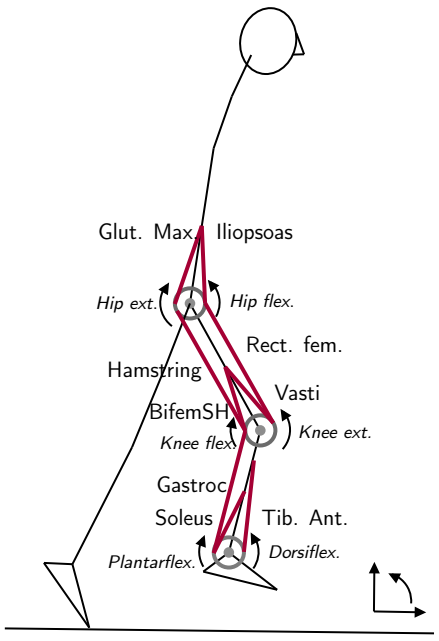

Figure 3: H0920. The gastrocnemius was split up into its medial and lateral parts.

H0920 is a 2D model with 9 degrees of freedom. From the ground up: rotation around the frontal axis at the pelvis and the ankle, knee, and hip for both legs, as well as translation in the sagittal and vertical planes. The model is actuated with 20 Hill-type muscles.[66] The maximum isometric muscle forces are based on Rajagopal et al. [61] and the muscle parameters are based on the OpenSim Gait1018 model.[53] H0920 represents a male adult of 75kg and 1.80. An overview is shown in Figure 3.

The feet are modeled with two contact spheres in each foot, one located at the heel and one located at the toes. Both spheres have a radius of 3 cm and a stiffness of 17461 MPa. To optimize computational efficiency and avoid unnecessary complexity, all elements within the model were kept simple. This enabled a more focused investigation of the effects of the different model components on the simulated kinematics. The model was created in HyFyDy, a SCONE-compatible software package, enabling faster simulation runtimes.[67]

Objective function

The objective function used in H0920_RUN incorporated a cost-of-transport term based on Uchida et al. [68]. This effort model was specifically designed for use in muscle-driven models of running. Additionally, the objective included a velocity term that becomes zero when the pelvis center of mass (COM) has a forward velocity of 3 m/s, evaluated per step. This corresponds to the pace of an endurance run. The goal was to minimize the outcome of the objective function.

Controller

The controller in H0920_RUN is a neural reflex controller and incorporates monosynaptic and antagonistic muscle force and length feedback. This applies to each muscle. The gait cycle was not split up into separate control phases. Collectively this reflex-based controller looks as follows:

$$A_{muscle} = C_0 + K_F * F_{muscle} + K_l * l_{muscle} + K_{F_{ant}} * F_{antagonist} + K_{l_{ant}} * l_{antagonist} \quad (1)$$

Where A_{muscle} is the muscle activation, C_0 is the offset, K_F and K_l are the force and length reflex gains respectively. C_0, K_F and K_l are the parameters used in the optimization. A complete overview is given in Appendix A. These control parameters were optimized using a shooting-based method.[67] The neural latencies used in this model were taken from Van der Kruk and Geijtenbeek [49]. These are more in line with realistic delays than the ones used in previous studies.

The simulation that resulted from the H0920_RUN is referred to as S_H0920_RUN. The adaptations that were made to H0920_RUN to test each hypothesis are listed below.

H_MSK1 (model S_MSK1) In S_MSK1, a toe joint was added to H0920_RUN. This joint was modeled as a passive pure rotational joint around the frontal axis of the first metatarsophalangeal joint of the big toe. The joint had a stiffness of 25 Nm/rad, and a damping of 2 Nms/rad, similar to the toe joint in Falisse et al. [47].

H_MSK2 (model S_MSK2) The stiffness of the Achilles tendon was decreased by 60% when compared to H0920_RUN, resulting in S_MSK2. This was done by setting the HyFyDy stiffness multiplier to 0.4 for both the gastrocnemius and the soleus muscles on both sides.

H_MSK3 (model S_MSK3) A thoracic and a lumbar joint were added to H0920, resulting in S_MSK3. The thoracic joint was located between the most superior lumbar vertebra and the most inferior thoracic vertebra and allowed for rotation around the frontal axis. The lumbar joint allowed rotation around the frontal axis between the pelvis and inferior lumbar vertebra. Both joints were torque-driven, with a maximum actuation of 1000 N/m. Additionally, a joint torque penalty was added to the objective function to account for the energy use of the lacking upper body muscles.

H_MSK4 (model S_MSK4) S_MSK4 incorporated the muscle parameters from the OpenSim Gait2392 model[60] and the updated ones proposed by Rajagopal et al. [61] in H0920_RUN.

H_MSK5 (model S_MSK5) The maximum isometric forces from the OpenSim Gait2392 model[60] were implemented in S_MSK4. This resulted in S_MSK5. In general, the maximum isometric forces from the OpenSim Gait2392 model[53] were lower than the forces in Rajagopal et al. [61]. As a result, H_0920_RUN with maximum isometric forces based on the OpenSim Gait2392 model[53] did not have enough muscle strength to reach a stable running gait cycle (Appendix C). The muscle force differences between both models were not consistent and ranged from 112% higher for the vasti muscle group in H0920 to 30% lower for both the tibialis anterior and biceps femoris short head. To test the influence of the ratio of maximum isometric forces, while also having enough muscle strength, the values in Delp et al. [53] were doubled and implemented in H_0920_RUN. This resulted in S_MSK5.

H_FC1 (model S_FC1a & S_FC1b) H_FC1 was tested by creating one model with a foot contact sphere stiffness of 1000% (S_FC1a), creating a practically rigid foot, and one with a contact sphere stiffness of 25%(S_FC1b) compared to the stiffness of 17461MPa in H0920_RUN. The results of both simulations were compared to each other.

H_O1 (model S_O1) The cost-of-transfer term in the objective function of H0920_RUN was replaced with a squared muscle activation term, resulting in S_O1. The resulting kinematics of S_O1 and S_H0920_RUN were compared with the kinematics of S_H0920_RUN to determine which objective function resulted in more realistic knee stance kinematics.

H_O2 (model S_O2) In S_O2 both a squared muscle activation and a cost-of-transfer term were implemented in the objective function, similar to the objective function used in H1120_WALK. This implements a cost-of-transfer term based on Wang et al. [69]. The resulting kinematics were compared with S_O1 and S_H0920_RUN. For S_O1 and S_O2, no additional penalty terms were added.

H_O3 (model S_O3) H0920_RUN had a rigid torso-head connection, therefore torso instead of head accelerations were studied. This is in line with previous studies.[70] The peak magnitude of the torso acceleration in S_H0920_RUN was compared to the experimental data from Hamner and Delp [71]. If the peak magnitude in S_H0920_RUN was larger than the peak magnitude found in the experimental data, a penalty term was added to the objective function of H0920_RUN, resulting in S_O3. This penalty would go to zero when the torso acceleration fell below the peak magnitude found in the experimental data. If, on the other hand, the peak magnitudes in S_H0920_RUN fell below the peak magnitude found in the experimental data, the variable was not investigated further as a potential penalty term. A penalty term capped on the experimental peak magnitude would not influence the simulation performance if the peak was already lower in the simulated outcomes.

H_O4 (model S_O4) Similar to the approach for H_O3, the peak magnitude of the ground reaction force in S_H0920_RUN was compared to the experimental data from Hamner and Delp [71]. Furthermore, the same approach was used to determine whether the implementation of a penalty term was sensible by comparing the peak magnitude of the ground reaction force in S_H0920_RUN with the experimental data.

H_O5 (model S_O5) To test H_O5, the potential influence of a joint load penalty, first the simulated joint loads were increased. To this end, for S_FC1a, H0920_RUN was adapted with a foot contact sphere stiffness of 1000% of the original model's, making it practically rigid. In this scenario, less energy can be stored in the foot. This energy must be distributed in another way, which leads to increased joint load. Subsequently, for S_O5, a joint load penalty was added to the objective function of S_FC1a. This penalty term penalized ankle, knee, and hip loads above the magnitude of the loads calculated in S_FC1b, a low stiffness foot, and thus low joint load, scenario. For the experimental data, the joint loads were calculated with the joint reaction analysis in OpenSim using the CMC outcomes. For the simulated data, these were extracted from Scone.

H_C1 (model S_C1a & S_C1b) To test H_C1, a more unstable situation had to be created when compared to S_H0920_RUN. This induces the need for a more stable control strategy, which was hypothesized to induce knee flexion during stance. Instability can be caused by external or internal perturbations such as motor noise.[72] Motor noise includes all random signal disturbances that act on neural signals between the muscles and spinal cord and result in variability in the force that is generated by the muscle fibers. With increased motor noise, the effects of movements are more uncertain and a more variability-proof control mechanism must be found. Human motor behavior seems to be optimized to minimize the impact of motor noise.[72]. H_C1 was tested with two sources of instability: external perturbations (S_C1a) and motor noise (S_C1b).

The perturbations added in S_C1a were modeled as 400 N forces for 50 ms applied every second step at the foot in the posterior direction. This perturbation type was chosen to simulate tripping over unevenness in the running surface. Similar perturbations were added in Klemetti et al. [70] and John et al. [36]. The motor noise that was introduced in S_C1b had a baseline standard deviation of 0.10 and a proportional standard deviation of 1.0, by which the current signal is multiplied. This was the maximum noise level that could be added while still resulting in a stable gait pattern.

H_C2 (model S_C2) To simulate vestibular feedback, postural feedback reflexes were added to the controller used in H0920_RUN, resulting in S_C2. This was done by adding PD control for the iliopsoas, gluteus maximus, hamstrings, and rectus femoris muscles, based on the angle of the pelvis tilt. The goal orientation was an upright position.

H_C3 (model S_C3) H_C3, the effect of a multiphase controller could not be tested due to time constraints.

3.3 Verification

To test to what degree the simulation outcomes were biologically accurate, the outcomes of each simulation were compared to open-source experimental data collected by Hamner and Delp [71]. This data set consists of motion capture data, electromyography (EMG) data, and ground reaction forces of ten subjects running at 3.0 m/s. For each subject, one recording of 5 seconds was available. The subjects were experienced male long-distance runners (29 $\pm$ 5 yrs, 1.77 $\pm$ 0.04 m, 70.9 $\pm$ 7.0 kg), each running at least 50 kilometers a week. Seven of them were mid-to-rearfoot strikers and three were forefoot strikers.[71] The motion capture data was processed in OpenSim by Hamner and Delp [71] to obtain joint kinematics (using inverse kinematics (IK)), muscle activations and forces (using Computed Muscle Control (CMC)) and joint kinetics (using the residual reduction algorithm (RRA)).[53][71] For the joint kinematics the entire recording consisting of around 15 gait cycles was available. For the CMC and RRA results, only 3 gait cycles per subject were available.

4 Results

The baseline performance of both H1120_WALK and H0920_RUN is shown in Appendix B.

4.1 Musculoskeletal model

H_MSK1: Toe joint

The addition of a toe joint (S_MSK1) did not lead to an improvement of knee kinematics (Figure 4).

H_MSK2: Decreasing AT stiffness

Decreasing the Achilles tendon stiffness (S_MSK2) also did not lead to improvement of the knee kinematics (Figure 4). Therefore, H_MSK1 and H_MSK2 were rejected.

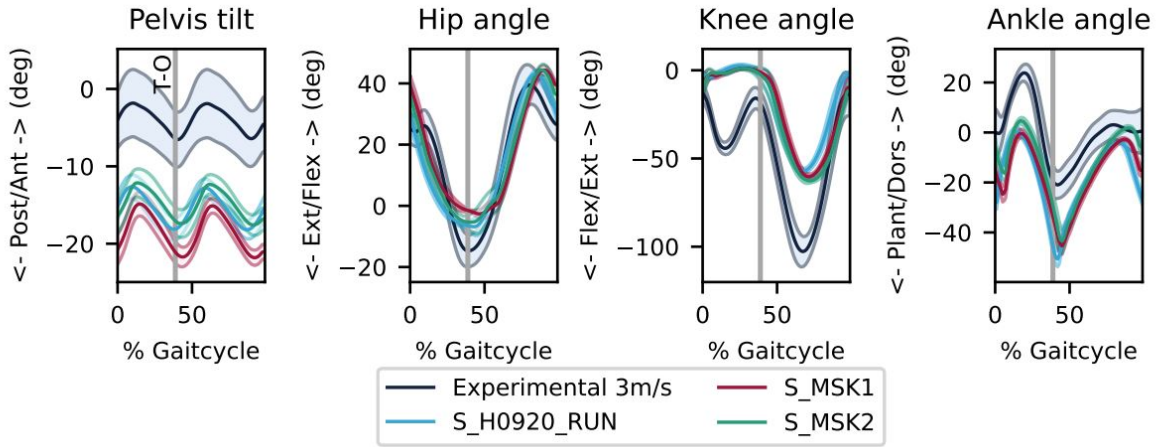

Figure 4: S_MSK1 features a toe joint, S_MSK2 features an Achilles tendon with decreased stiffness.

H_MSK3: Lumbar & thoracic joint

In S_MSK3, the pelvis kinematics had improved when compared to S_H0920_RUN, producing a pelvis tilt motion that was very similar to the experimentally observed pelvis tilt, as is shown in Figure 5. However, no subsequent improvement in knee kinematics was observed. Therefore, H_MSK3 was rejected.

H_MSK4: Muscle parameters

No improvement in stance knee kinematics was observed in S_MSK4 (Figure 5), leading to the rejection of H_MSK4.

H_MSK5: Maximum isometric forces

S_MSK5 did not show improved knee kinematics (Figure 5). Therefore, H_MSK5 was rejected.

H_FC1: Foot stiffness

An increased foot contact stiffness (S_FC1a) does not impact the knee stance kinematics, even when compared to a decreased stiffness scenario (S_FC1b) (Figure 6). This led to the rejection of H_FC1.

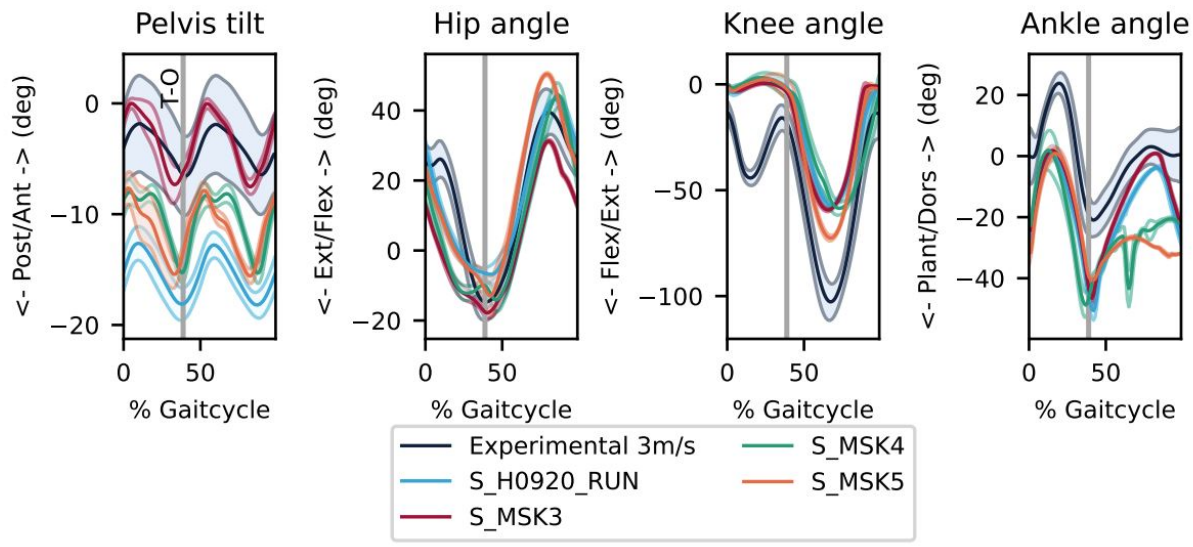

Figure 5: S_MSK3 is H0920_RUN with added lumbar and thoracic joints, S_MSK4 is H0920_RUN with muscle parameters from Delp et al. [60] and Rajagopal et al. [61]. In addition to this, S_MSK5 included the doubled maximum isometric forces from Delp et al. [53]

.

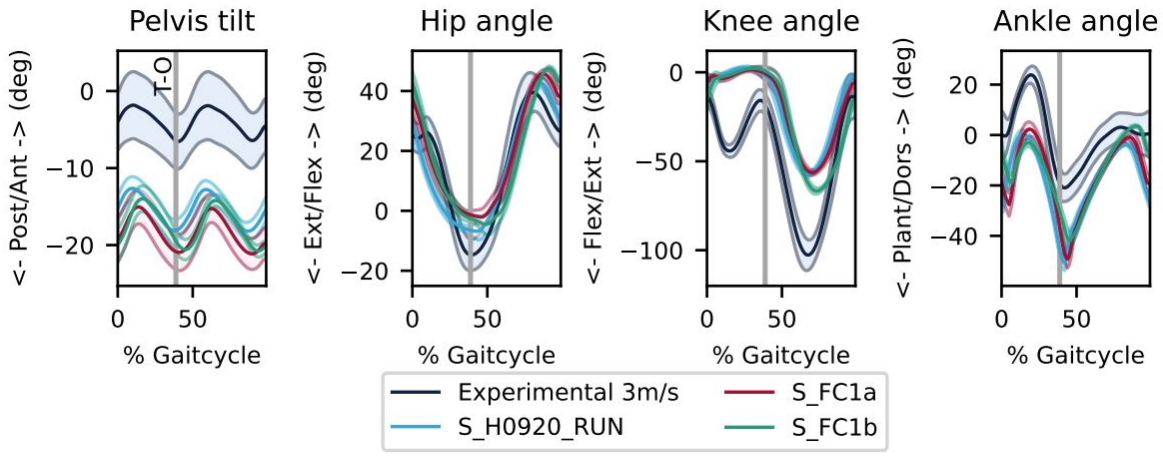

Figure 6: The effect of different foot contact stiffnesses. The low contact stiffness scenario (S_FC1b) had a contact stiffness of 25% of the baseline, the high stiffness model (S_FC1a) had a contact stiffness of 1000%

4.2 Objective function

H_O1,H_O2: Main objective

Changing the main objective from Cost-of-Transport to activation-based or a combination of both did not lead to improvements in the knee kinematics (Figure 7). Therefore H_O1 and H_O2 were rejected.

H_O3: Minimizing torso acceleration

The peak torso acceleration magnitude in the experimental running data was $18.60 \pm 2.14 m/s^2$, in H0920_RUN this was $14.55 \pm 4.01 m/s^2$. This is in line with results found in literature, where head accelerations have been shown to lie between 2-3g while running 3m/s.[73][74] This leads to the rejection of HO_3.

H_O4: Minimizing ground reaction force

The peak magnitudes of the GRF are lower in S_H0920_RUN when compared to the experimental data: GRF: 2.24±0.21 times bodyweight (xBW) vs 2.57±0.27 xBW. This led to the rejection of HO_4.

H_O5: Minimizing joint loads

As expected, the increased foot contact stiffness in S_FC1a led to increased ankle and knee joint load peak magnitudes of 8.75±0.49xBW and 7.83±0.39xBW respectively. Subsequently, joint load penalties were added at 7.4xBW and 6.3xBW in S_O4, equal to the peak joint load magnitudes observed in S_FC1b, the simulation with decreased foot contact stiffness. The load penalties in S_O5 did lead to a decrease in joint loads for both the ankle (7.34±0.39xBW) and the knee (6.29±0.28xBW). However, no improvement in lower limb kinematics was observed, which is shown in Figure 7. H_O5 was rejected.

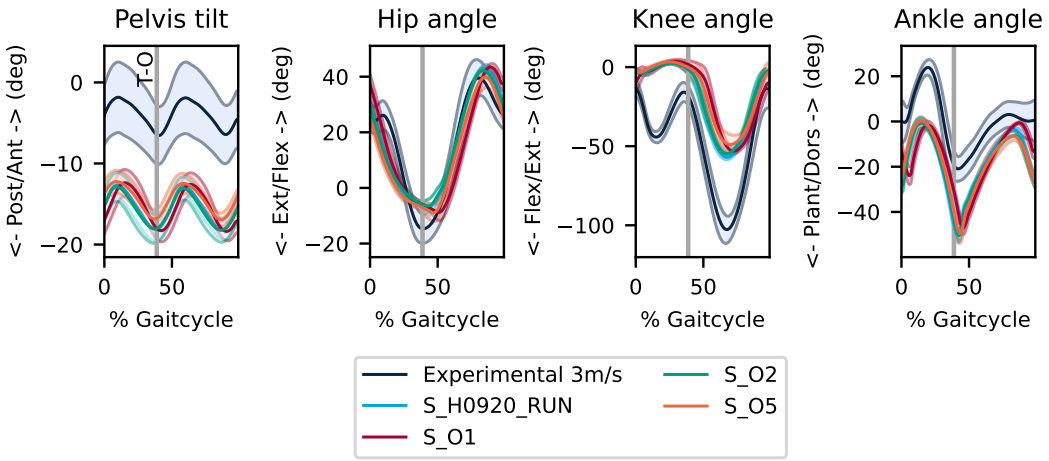

Figure 7: S_H0920_RUN has a COT objective, S_O1 a activation-based objective, S_O2 has combination. S_O5 features a joint load penalty and increased foot contact stiffness.

4.3 Controller

H_C1: stability

Both external (S_C1a) and internal (S_C1b) perturbations did not improve the stance knee kinematics (Figure 8), leading to the rejection of H_C1.

H_C2: Vestibular feedback

S_C2, adding vestibular feedback, did not improve the lower limb kinematics, see Figure 8. This led to the rejection of H_C2.

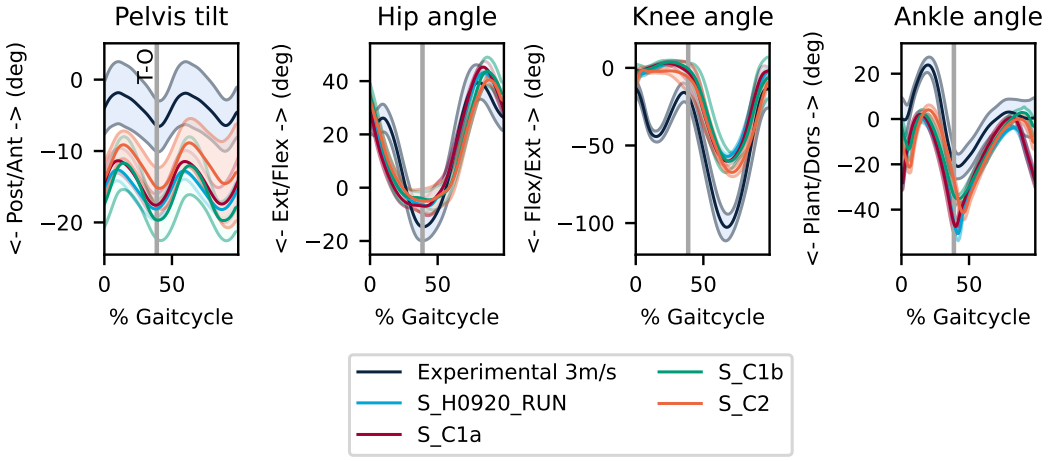

Figure 8: The influence of both external (S_C1a) and internal (S_C1b) perturbations on the joint kinematics. S_C2 shows the influence of added vestibular feedback.

5 Discussion

This study explored various hypotheses aimed at improving the stance phase knee kinematics in the predictive simulation of running. A structured analysis was performed, focusing on the complete predictive simulation framework, and analyzing the potential impact of modeling elements individually. In contrast to previous studies, adaptations to the musculoskeletal model or objective function resulted in no improvement in lower limb kinematics. After conducting extensive simulations, all but one hypothesis was rejected, with multiphase control remaining as the final non-tested hypothesis (Figure 9). Multiphase control is therefore considered the most likely element to be essential in simulating realistic knee flexion during stance.

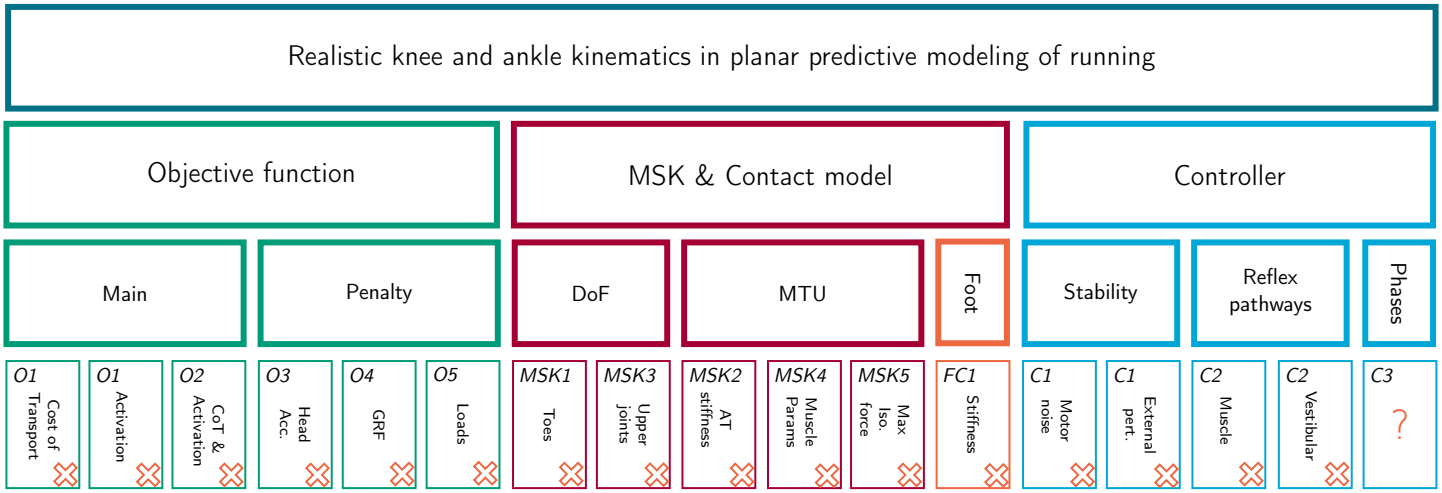

Figure 9: A complete overview of the elements that were tested for their influence on the ankle and knee kinematics in the predictive simulation of running. The hypotheses marked with a cross were rejected in this study.

In contrast to this current study, previous studies did find improvement in knee stancephase kinematics when implementing adaptations to the musculoskeletal model or the objective function. Falisse et al. [47], found an improvement in stance phase kinematics by adding a toe joint and reducing the Achilles tendon (AT) stiffness. Falisse et al. [47] made use of open-loop control, which might have led to the difference in results. By using 50 to 125 mesh intervals per half gait cycle, they essentially created multi-phase control. Open-loop control is however less suitable for studies investigating realistic human control and movement strategies as they disregard the role of sensory feedback.[39] In an experimental study by Hall and Nester [75], the flexibility of the foot and the metatarsal joints showed limited effects on stance phase kinematics. This is in line with the rejection of the hypotheses regarding the foot contact model in this study.

Furthermore, Veerkamp et al. [48] found an improvement in stance phase kinematics when implementing an extensive objective function with COT and activation-based terms as well as ground reaction force and acceleration penalty terms. This current study did not find such an improvement. This study primarily tested individual elements, the effects of subsystem combinations and modeling choices were not examined. It is possible that the interacting effects between subsystems were overlooked. For example, a change in the MSK model could result in an increase in GRF, which could be counteracted by a GRF penalty. This, in turn, might result in a change in kinematics. A sensitivity analysis could be performed to determine the influence of different modeling elements on each other. However, since none of the tested model components had any effect on the degree of stance knee flexion, it is unlikely that a combination would lead to large differences in simulated knee kinematics. Veerkamp et al. [48] made use of multiphase control. Adaptations to the objective function or the MSK model may lead to further improvement in knee kinematics when the multiphase condition is met.

The build-up of predictive models is often unclear, with many submodels and hidden modeling choices that might influence results. Future studies should keep in mind that this not only limits the repeatability of these studies but also limits their potential applicability in a more practical or clinical setting and the collaboration between different research fields.

One important limitation of this study is that the influence of the maximum isometric force could not be directly tested. This was due to the muscle parameters being too weak to get to a running motion. While the muscle parameters and forces seem to have little influence on the predicted kinematics, it is important to make sure that when investigating the running motion, the maximum isometric forces that are used in the model are capable of running. The "true" value of these maximum isometric forces, and other muscle parameters, remains an ongoing research area in musculoskeletal modeling.[31] The effect of the uncertainty in these parameters could influence the outcomes of predictive models of human movement. This limits the accuracy of outcomes, and therefore their usefulness in clinical applications.

Another limitation was the algorithm that is used in the optimizations is an evolutionary algorithm, which is sensitive to local optima.[76] This probably caused the gait pattern in S_MSK4, in which the toe tapped the ground during swing phase. This is not a realistic gait pattern, and while a variety of initial states were tried, the algorithm consistently found this particular pattern. To increase the chances of finding the global optimum, it is recommended to use a higher number of parallel optimizations, with a wider initial parameter space.

This study focused on two-dimensional predictive simulation of gait. The results show that an increased need for stability did not affect the knee kinematics in 2D simulations. This finding is consistent with Bauby and Kuo [77], where it was demonstrated that fore-aft balance is primarily caused by the passive dynamics of the leg. Fore-aft balance can be achieved in a two-legged model without knees and sensory feedback.[78] In contrast, some form of active feedback control is necessary for medial-lateral balance.[77]

The objective of the optimization algorithm is to minimize metabolic energy while finding a stable gait pattern. In two-dimensional simulation, a stable gait pattern does not require active feedback control. Therefore, in this case, the most important element for the controller is minimizing metabolic energy. Knee flexion could increase stability, but in two-dimensional models, no energy has to be used to maintain medial-lateral balance. Throughout the simulations performed in this study, no activation of the knee flexors and extensors was seen (Appendix E). In a three-dimensional model, the need for medial-lateral stability is introduced, which requires active feedback control. Finding a stable gait pattern is prioritized over minimizing metabolic energy. The cost of activating the muscles that cause stance knee flexion outweighs the induced stability. Due to time constraints, H_0920_RUN was not expanded to 3D. However, it is expected that a stable, three-dimensional model, inherently shows knee flexion.

Even in a three-dimensional model, a multiphase controller is essential in simulating realistic knee kinematics. Throughout all simulations, very limited changes to the knee and ankle kinematics were observed. In almost all simulations, the muscle activations of the biceps femoris short head, rectus femoris, and vasti muscles, causing knee flexion and extension, were zero throughout the entire gait cycle. When analyzing the activation patterns that would lead to realistic kinematics, the vasti and rectus femoris muscles show separate activation peaks during stance and swing.[71] For the biceps femoris short head, this information was not available. The activation peak during stance does not coincide with the peaks of either the muscle force or length, which are used to calculate the activation (Figure 10).[71][79] By increasing the offset, C0, or the feedback gains, KL or KF, lower values of muscle length and force could lead to activation of the muscles, and thus to an activation peak during stance. However, increasing the values of these parameters for the entire gait cycle would lead to increased activation of these muscles during early swing. This would cause rapid knee extension during early swing, which is expected to cause an unstable gait cycle. This can be countered by calculating different values of C0, KL and KF for separate phases in the gait cycle, and strengthens the idea that a realistic, stable, gait cannot be achieved using a single-phase reflex controller, in both 2D and 3D.

In humans, reflexes are modulated or even inhibited throughout the gait cycle. The dependence of the vestibular signals can be tested experimentally by analyzing the coherence of electrical vestibular stimulation (EVS) with muscle activity and ground reaction forces. The coherence between EVS and individual muscle activity peaks at different moments in the gait cycle.[58][80] Vestibular feedback can even be inhibited per muscle.[58] The modulation of these reflex gains and inhibition of reflexes is highly dependent on the task.[58][81][82]

In predictive simulations of gait, the modulation and inhibition of reflexes are captured in multiphase

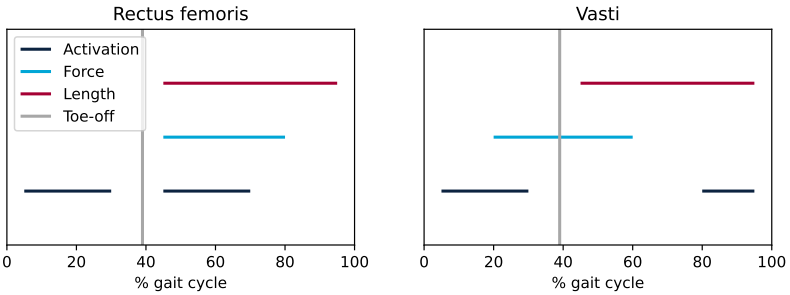

Figure 10: The timing of the peaks of the activation, force and length of the rectus femoris and vasti muscles. The activation and force data is from [71]. The muscle fiber length data is from Arnold et al. [79].

control. For each phase, the feedback gains can be determined separately and different feedback pathways can be present. The amount of phases, and which pathways are present per phase is mostly based on previous studies and iterative design.[49][83][84] In previous predictive simulations of gait, the gait cycle has been split up into as little as two (stance & swing [84]), to as much as five phases (early stance, late stance, lift-off, swing, landing)[48]. With two-phase control, already realistic gait knee kinematics can be realized.[84]

Often, the separation of the phases in predictive simulations is determined by kinematic or kinetic variables, such as ground reaction forces, segment positions, and joint angles.[83][84] In contrast, Song and Geyer [85] added a supraspinal control layer to initiate a smoother transition between stance and swing phases.[85] Research on sit-to-walk transitions shows that the transitions based on kinematic variables do not necessarily coincide with the transitions determined when optimizing for biological controls.[49] In gait, humans seem to use foot loading as a phase transition indicator [86], but it is unsure which other variables are used. Some form of active step-by-step modulation based on environmental variables and sensor input might be present. When the goal is to investigate the response to differences in environment and task, it would be interesting to investigate an algorithm that would determine the phases, their transitions, and the present pathways for the gait cycle automatically to more accurately simulate human sensorimotor behavior. A first step would be to find the gait cycle phase design for stable, non-disturbed, walking and running and then to extend that to scenarios with disturbances. However, this kind of (semi)-active control is probably still far away. A first step could be identifying the variables humans use to determine the transition and modulation of reflexes from one phase to another, specifically in running, to apply these more accurate phase designs in the predictive simulation framework. This could be done by either using human research using EVS or by applying multiple scenarios in predictive simulation.

Song and Geyer [85] developed a reflex controller that could predict multiple stable locomotion modes such as walking with different speeds and disturbances, including stairs and turns. However, their controller failed to find a stable running gait pattern, indicating that running and walking come from different reflex control designs. While both walking and running gait cycles can be split up in a stance and a swing phase for each leg, there are also inherent differences between walking and running gait cycles, with a double support and a no support phase respectively. Specifically during stance, the leg behaves like an inverted pendulum in walking, while showing more flexion and storage of elastic energy in running.[44]

Duysens et al. [86] shows increased cutaneous reflexes during running, while Edamura et al. [87] found decreased H-reflexes in running when compared to walking, independent of speed. EMG results suggest that the biggest difference in muscle activation timing between walking and running is found during stance, but that the number of phases is similar.[44] Additionally, Courtine et al. [88] found that running showed an anticipatory monosynaptic muscle reflex response shortly before the stance phase that was not present in walking, indicating that the sensorimotor phase transitions for walking and running lie at a different point in the gait cycle.

Collectively, it is not possible to directly extend walking reflexive control to running and expect biologically accurate running patterns. The main focus when extending a walking controller to running should lie on the timing of the phases and the present pathways during, and shortly before, stance.

6 Conclusion

Achieving realistic knee kinematics during the stance phase of running in a predictive neuromusculoskeletal model is a challenging task. A structured analysis of potentially influencing elements showed that adaptations to the musculoskeletal model, foot contact model, and objective function have negligible effects on the simulated stance knee kinematics in predictive simulations of running, in contrast to previous studies. The implementation of multiphase control is therefore considered essential in creating realistic knee and stance phase kinematics in planar predictive simulation of walking and running when using neural reflex control. Future research on improving the biomechanical accuracy of predictive models should therefore focus on the controller design. Not only into which phases and transitions, but also the level of active control in human movement control. On top of that, they should focus on clear communication and transparency of modeling choices for better cooperation between different study fields and in that way getting closer to applying predictive models in a clinical setting.

References

[1] S. Korbee, J. Bosch, and S. de Kort, "Zo sport Nederland Trends & ontwikkelingen in sportdeelname (2013-2018)," NOCNSF, Tech. Rep. NOC NSF 791, 2018.

[2] "2022 Outdoor Participation Trends Report," Outdoor Foundation, Tech. Rep., 2022.

[3] L. Audickas, "Sport participation in England," House of Commons Library, Tech. Rep. CBP 8181, Dec. 2017.

[4] R. M. Hulteen, J. J. Smith, P. J. Morgan, L. M. Barnett, P. C. Hallal, K. Colyvas, and D. R. Lubans, "Global participation in sport and leisure-time physical activities: A systematic review and meta-analysis," *Preventive Medicine*, vol. 95, pp. 14–25, Feb. 2017. [Online]. Available: https://www.sciencedirect.com/science/article/pii/S0091743516303838

[5] M. L. Ceravolo, J. E. Gaida, and R. J. Keegan, "Quality-of-Life in Achilles Tendinopathy: An Exploratory Study," *Clinical Journal of Sport Medicine*, vol. 30, no. 5, p. 495, Sep. 2020. [Online]. Available: https://journals.lww.com/cjsportsmed/Fulltext/2020/09000/Quality_of_Life_in_Achilles_Tendinopathy__An.11.aspx

[6] J. Verges, N. Martínez, A. Pascual, M. Bibas, M. Santiña, and G. Rodas, "Psychosocial and individual factors affecting Quality of Life (QoL) in patients suffering from Achilles tendinopathy: a systematic review," *BMC Musculoskeletal Disorders*, vol. 23, no. 1, p. 1114, Dec. 2022. [Online]. Available: https://doi.org/10.1186/s12891-022-06090-2

[7] N. P. Pronk, E. G. Bender, and A. S. Katz, "The 2018 Physical Activity Guidelines for Americans II: Associations between Social Determinants of Health and Meeting Guidelines for Physical Activity Among Employees," *ACSM'S Health & Fitness Journal*, vol. 23, no. 5, pp. 57–62, Sep. 2019. [Online]. Available: https://journals.lww.com/10.1249/FIT.0000000000000503

[8] A. D. Lopes, L. C. Hespanhol, S. S. Yeung, and L. O. P. Costa, "What are the Main Running-Related Musculoskeletal Injuries?" *Sports Medicine*, vol. 42, no. 10, pp. 891–905, Oct. 2012. [Online]. Available: https://doi.org/10.1007/BF03262301

[9] N. Kakouris, N. Yener, and D. T. P. Fong, "A systematic review of running-related musculoskeletal injuries in runners," *Journal of Sport and Health Science*, vol. 10, no. 5, pp. 513–522, Sep. 2021. [Online]. Available: https://www.sciencedirect.com/science/article/pii/S2095254621000454

[10] K. Knobloch, U. Yoon, and P. M. Vogt, "Acute and Overuse Injuries Correlated to Hours of Training in Master Running Athletes," *Foot & Ankle International*, vol. 29, no. 7, pp. 671–676, Jul. 2008, publisher: SAGE Publications Inc. [Online]. Available: https://doi.org/10.3113/FAI.2008.0671

[11] F. Di Caprio, R. Buda, M. Mosca, A. Calabro', and S. Giannini, "Foot and Lower Limb Diseases in Runners: Assessment of Risk Factors," *Journal of Sports Science & Medicine*, vol. 9, no. 4, pp. 587–596, Dec. 2010. [Online]. Available: https://www.ncbi.nlm.nih.gov/pmc/articles/PMC3761810/

[12] J. Sinclair, J. Richards, and H. Shore, "Effects of minimalist and maximalist footwear on Achilles tendon load in recreational runners," *Comparative Exercise Physiology*, vol. 11, no. 4, pp. 239–244, Dec. 2015, publisher: Wageningen Academic Publishers. [Online]. Available: https://www.wageningenacademic.com/doi/abs/10.3920/CEP150024

[13] Y. Zhang, Z. Chen, H. Zhao, X. Liang, C. Sun, and Z. Jin, "Musculoskeletal modeling of total ankle arthroplasty using force-dependent kinematics for predicting in vivo joint mechanics," *Proceedings of the Institution of Mechanical Engineers, Part H: Journal of Engineering in Medicine*, vol. 234, no. 2, pp. 210–222, Feb. 2020, publisher: IMECHE. [Online]. Available: https://doi.org/10.1177/0954411919890724

[14] H. Rice and M. Patel, "Manipulation of Foot Strike and Footwear Increases Achilles Tendon Loading During Running," *The American Journal of Sports Medicine*, vol. 45, no. 10, pp. 2411–2417, Aug. 2017.

[15] J. Hannigan and C. D. Pollard, "Differences in running biomechanics between a maximal, traditional, and minimal running shoe," *Journal of Science and Medicine in Sport*, vol. 23, no. 1, pp. 15–19, Jan. 2020. [Online]. Available: https://linkinghub.elsevier.com/retrieve/pii/S1440244019304736

[16] S. M. Marberry, S. E. Filmalter, G. G. Pujalte, J. C. Presley, K. F. DeMatas, D. P. Montero, K. Israni, C. T. Ball, and J. R. Maynard, "Self-reported foot strike patterns and sonographic evidence of Achilles tendinopathy in asymptomatic marathon runners," *Journal of Sports Sciences*, vol. 40, no. 12, pp. 1308–1314, Jun. 2022, publisher: Routledge _eprint: https://doi.org/10.1080/02640414.2022.2080158. [Online]. Available: https://doi.org/10.1080/02640414.2022.2080158

[17] D. S. B. Williams, J. A. Zambardino, and V. A. Banning, "Transverse-plane mechanics at the knee and tibia in runners with and without a history of achilles tendonopathy," *The Journal of Orthopaedic and Sports Physical Therapy*, vol. 38, no. 12, pp. 761–767, Dec. 2008.

[18] R. W. Willy and M. R. Paquette, "The Physiology and Biomechanics of the Master Runner," *Sports Medicine and Arthroscopy Review*, vol. 27, no. 1, pp. 15–21, Mar. 2019, place: Philadelphia Publisher: Lippincott Williams & Wilkins WOS:000458333000005. [Online]. Available: https://www.webofscience.com/wos/woscc/summary/c61d9456-db3b-4a06-b2d3-b74e31534586-6b574073/relevance/8

[19] Y. Haglund-Åkerlind and E. Eriksson, "Range of motion, muscle torque and training habits in runners with and without Achilles tendon problems," *Knee Surgery, Sports Traumatology, Arthroscopy*, vol. 1, no. 3, pp. 195–199, Sep. 1993. [Online]. Available: https://doi.org/10.1007/BF01560205

[20] C. A. Reule, W. W. Alt, H. Lohrer, and H. Hochwald, "Spatial orientation of the subtalar joint axis is different in subjects with and without Achilles tendon disorders," *British Journal of Sports Medicine*, vol. 45, no. 13, pp. 1029–1034, Oct. 2011.

[21] U. Waldecker, G. Hofmann, and S. Drewitz, "Epidemiologic investigation of 1394 feet: Coincidence of hindfoot malalignment and Achilles tendon disorders," *Foot and Ankle Surgery*, vol. 18, no. 2, pp. 119–123, Jun. 2012. [Online]. Available: https://www.sciencedirect.com/science/article/pii/S1268773111000695

[22] K. R. Kaufman, S. K. Brodine, R. A. Shaffer, C. W. Johnson, and T. R. Cullison, "The Effect of Foot Structure and Range of Motion on Musculoskeletal Overuse Injuries," *The American Journal of Sports Medicine*, vol. 27, no. 5, pp. 585–593, Sep. 1999, publisher: SAGE Publications Inc STM. [Online]. Available: https://doi.org/10.1177/03635465990270050701

[23] D. Clement, J. Taunton, and G. Smart, "Achilles tendinitis and peritendinitis: Etiology and treatment," *The American Journal of Sports Medicine*, vol. 12, no. 3, pp. 179–184, May 1984, publisher: SAGE Publications Inc STM. [Online]. Available: https://doi.org/10.1177/036354658401200301

[24] N. N. Mahieu, E. Witvrouw, V. Stevens, D. Van Tiggelen, and P. Roget, "Intrinsic Risk Factors for the Development of Achilles Tendon Overuse Injury: A Prospective Study," *The American Journal of Sports Medicine*, vol. 34, no. 2, pp. 226–235, Feb. 2006, publisher: SAGE Publications Inc STM. [Online]. Available: https://doi.org/10.1177/0363546505279918

[25] W. Hansen, V. B. Shim, S. Obst, D. G. Lloyd, R. Newsham-West, and R. S. Barrett, "Achilles tendon stress is more sensitive to subject-specific geometry than subject-specific material properties: A finite element analysis," *Journal of Biomechanics*, vol. 56, pp. 26–31, May 2017. [Online]. Available: https://www.sciencedirect.com/science/article/pii/S002192901730132X

[26] G. G. Handsfield, J. Greiner, J. Madl, E. A. Rog-Zielinska, E. Hollville, B. Vanwanseele, and V. Shim, "Achilles Subtendon Structure and Behavior as Evidenced From Tendon Imaging and Computational Modeling," *Frontiers in Sports and Active Living*, vol. 2, 2020. [Online]. Available: https://www.frontiersin.org/articles/10.3389/fspor.2020.00070

[27] V. B. Shim, W. Hansen, R. Newsham-West, L. Nuri, S. Obst, C. Pizzolato, D. G. Lloyd, and R. S. Barrett, "Influence of altered geometry and material properties on tissue stress distribution under load in tendinopathic Achilles tendons – A subject-specific finite element analysis," *Journal of Biomechanics*, vol. 82, pp. 142–148, Jan. 2019. [Online]. Available: https://www.sciencedirect.com/science/article/pii/S0021929018308042

[28] E. A. Schmida, C. M. Wille, M. R. Stiffler-Joachim, S. A. Kliethermes, and B. C. Heiderscheit, "Vertical Loading Rate Is not Associated with Running Injury, Regardless of Calculation Method," *Medicine and science in sports and exercise*, vol. 54, no. 8, pp. 1382–1388, Aug. 2022. [Online]. Available: https://www.ncbi.nlm.nih.gov/pmc/articles/PMC9288487/

[29] B. D. Rooney and T. R. Derrick, "Joint contact loading in forefoot and rearfoot strike patterns during running," *Journal of Biomechanics*, vol. 46, no. 13, pp. 2201–2206, Sep. 2013. [Online]. Available: https://www.sciencedirect.com/science/article/pii/S0021929013002960

[30] C. Napier, C. L. MacLean, J. Maurer, J. E. Taunton, and M. A. Hunt, "Kinetic risk factors of running-related injuries in female recreational runners," *Scandinavian Journal of Medicine & Science in Sports*, vol. 28, no. 10, pp. 2164–2172, Oct. 2018.

[31] S. D. Uhlrich, T. K. Uchida, M. R. Lee, and S. L. Delp, "Ten steps to becoming a musculoskeletal simulation expert: A half-century of progress and outlook for the future," *Journal of Biomechanics*, vol. 154, p. 111623, Jun. 2023. [Online]. Available: https://www.sciencedirect.com/science/article/pii/S0021929023001926

[32] H. Geyer, A. Seyfarth, and R. Blickhan, "Compliant leg behaviour explains basic dynamics of walking and running," *Proceedings of the Royal Society B: Biological Sciences*, vol. 273, no. 1603, pp. 2861–2867, Aug. 2006, publisher: Royal Society. [Online]. Available: https://royalsocietypublishing.org/doi/10.1098/rspb.2006.3637

[33] A. D. Kuo, "The six determinants of gait and the inverted pendulum analogy: A dynamic walking perspective," *Human Movement Science*, vol. 26, no. 4, pp. 617–656, Aug. 2007. [Online]. Available: https://www.sciencedirect.com/science/article/pii/S0167945707000309

[34] M. Srinivasan and A. Ruina, "Computer optimization of a minimal biped model discovers walking and running," *Nature*, vol. 439, no. 7072, pp. 72–75, Jan. 2006, number: 7072 Publisher: Nature Publishing Group. [Online]. Available: https://www.nature.com/articles/nature04113

[35] R. H. Miller, "A comparison of muscle energy models for simulating human walking in three dimensions," *Journal of Biomechanics*, vol. 47, no. 6, pp. 1373–1381, Apr. 2014. [Online]. Available: https://www.sciencedirect.com/science/article/pii/S0021929014000876

[36] C. T. John, F. C. Anderson, J. S. Higginson, and S. L. Delp, "Stabilisation of walking by intrinsic muscle properties revealed in a three-dimensional muscle-driven simulation," *Computer Methods in Biomechanics and Biomedical Engineering*, vol. 16, no. 4, pp. 451–462, Apr. 2013, publisher: Taylor & Francis _eprint: https://doi.org/10.1080/10255842.2011.627560. [Online]. Available: https://doi.org/10.1080/10255842.2011.627560

[37] N. F. J. Waterval, M. A. Brehm, K. Veerkamp, T. Geijtenbeek, J. Harlaar, F. Nollet, and M. M. van der Krogt, "Interacting effects of AFO stiffness, neutral angle and footplate stiffness on gait in case of plantarflexor weakness: A predictive simulation study," *Journal of Biomechanics*, vol. 157, p. 111730, Aug. 2023. [Online]. Available: https://www.sciencedirect.com/science/article/pii/S0021929023002993

[38] C. F. Ong, T. Geijtenbeek, J. L. Hicks, and S. L. Delp, "Predicting gait adaptations due to ankle plantarflexor muscle weakness and contracture using physics-based musculoskeletal simulations," *PLOS Computational Biology*, vol. 15, no. 10, p. e1006993, 2019, publisher: Public Library of Science. [Online]. Available: https://journals.plos.org/ploscompbiol/article?id=10.1371/journal.pcbi.1006993

[39] A. Falisse, G. Serrancolí, C. L. Dembia, J. Gillis, I. Jonkers, and F. De Groote, "Rapid predictive simulations with complex musculoskeletal models suggest that diverse healthy and pathological human gaits can emerge from similar control strategies," *Journal of The Royal Society Interface*, vol. 16, no. 157, p. 20190402, Aug. 2019, publisher: Royal Society. [Online]. Available: https://royalsocietypublishing.org/doi/10.1098/rsif.2019.0402

[40] J. Shanbhag, A. Wolf, I. Wechsler, S. Fleischmann, J. Winkler, S. Leyendecker, B. M. Eskofier, A. D. Koelewijn, S. Wartzack, and J. Miehling, "Methods for integrating postural control into biomechanical human simulations: a systematic review," *Journal of NeuroEngineering and Rehabilitation*, vol. 20, no. 1, p. 111, Aug. 2023. [Online]. Available: https://doi.org/10.1186/s12984-023-01235-3

[41] A. D. Kuo, "An optimal state estimation model of sensory integration in human postural balance," *Journal of Neural Engineering*, vol. 2, no. 3, p. S235, Aug. 2005. [Online]. Available: https://dx.doi.org/10.1088/1741-2560/2/3/S07

[42] A. J. Van den Bogert, M. Hupperets, H. Schlarb, and B. Krabbe, "Predictive musculoskeletal simulation using optimal control: effects of added limb mass on energy cost and kinematics of walking and running," *Proceedings of the Institution of Mechanical Engineers, Part P: Journal of Sports Engineering and Technology*, vol. 226, no. 2, pp. 123–133, Jun. 2012, publisher: SAGE Publications. [Online]. Available: https://doi.org/10.1177/1754337112440644

[43] H.-M. Maus, S. Revzen, J. Guckenheimer, C. Ludwig, J. Reger, and A. Seyfarth, "Constructing predictive models of human running," *Journal of The Royal Society Interface*, vol. 12, no. 103, p. 20140899, Feb. 2015, publisher: Royal Society. [Online]. Available: https://royalsocietypublishing.org/doi/full/10.1098/rsif.2014.0899

[44] G. Cappellini, Y. P. Ivanenko, R. E. Poppele, and F. Lacquaniti, "Motor Patterns in Human Walking and Running," *Journal of Neurophysiology*, vol. 95, no. 6, pp. 3426–3437, Jun. 2006, publisher: American Physiological Society. [Online]. Available: https://journals.physiology.org/doi/full/10.1152/jn.00081.2006

[45] M. Voigt and E. A. Hansen, "The puzzle of the walk-to-run transition in humans," *Gait & Posture*, vol. 86, pp. 319–326, May 2021. [Online]. Available: https://www.sciencedirect.com/science/article/pii/S096663622100120X

[46] M. G. J. Gazendam and A. L. Hof, "Averaged EMG profiles in jogging and running at different speeds," *Gait & Posture*, vol. 25, no. 4, pp. 604–614, Apr. 2007. [Online]. Available: https://www.sciencedirect.com/science/article/pii/S0966636206001408

[47] A. Falisse, M. Afschrift, and F. D. Groote, "Modeling toes contributes to realistic stance knee mechanics in three-dimensional predictive simulations of walking," *PLOS ONE*, vol. 17, no. 1, p. e0256311, Jan. 2022, publisher: Public Library of Science. [Online]. Available: https://journals.plos.org/plosone/article?id=10.1371/journal.pone.0256311

[48] K. Veerkamp, N. F. J. Waterval, T. Geijtenbeek, C. P. Carty, D. G. Lloyd, J. Harlaar, and M. M. van der Krogt, "Evaluating cost function criteria in predicting healthy gait," *Journal of Biomechanics*, vol. 123, p. 110530, Jun. 2021. [Online]. Available: https://www.sciencedirect.com/science/article/pii/S0021929021003110

[49] E. Van der Kruk and T. Geijtenbeek, "A planar neuromuscular controller to simulate age-related adaptation strategies in the sit-to-walk movement." 2023.

[50] F. De Groote and A. Falisse, "Perspective on musculoskeletal modelling and predictive simulations of human movement to assess the neuromechanics of gait," *Proceedings of the Royal Society B: Biological Sciences*, vol. 288, no. 1946, p. 20202432, Mar. 2021, publisher: Royal Society. [Online]. Available: https://royalsocietypublishing.org/doi/full/10.1098/rspb.2020.2432

[51] R. H. Miller, B. R. Umberger, J. Hamill, and G. E. Caldwell, "Evaluation of the minimum energy hypothesis and other potential optimality criteria for human running," *Proceedings of the Royal Society B: Biological Sciences*, vol. 279, no. 1733, pp. 1498–1505, Nov. 2011, publisher: Royal Society. [Online]. Available: https://royalsocietypublishing.org/doi/10.1098/rspb.2011.2015

[52] M. Millard and K. Mombaur, "A Quick Turn of Foot: Rigid Foot-Ground Contact Models for Human Motion Prediction," *Frontiers in Neurorobotics*, vol. 13, 2019. [Online]. Available: https://www.frontiersin.org/articles/10.3389/fnbot.2019.00062

[53] S. L. Delp, F. C. Anderson, A. S. Arnold, P. Loan, A. Habib, C. T. John, E. Guendelman, and D. G. Thelen, "OpenSim: open-source software to create and analyze dynamic simulations of movement," *IEEE transactions on bio-medical engineering*, vol. 54, no. 11, pp. 1940–1950, Nov. 2007.

[54] K. Harms-Ringdahl, A. M. Carlsson, J. Ekholm, A. Raustorp, T. Svensson, and H.-G. Toresson, "Pain assessment with different intensity scales in response to loading of joint structures," *Pain*, vol. 27, no. 3, pp. 401–411, Dec. 1986. [Online]. Available: https://www.sciencedirect.com/science/article/pii/0304395986901636

[55] B. I. Prilutsky and V. M. Zatsiorsky, "Tendon action of two-joint muscles: Transfer of mechanical energy between joints during jumping, landing, and running," *Journal of Biomechanics*, vol. 27, no. 1, pp. 25–34, Jan. 1994. [Online]. Available: https://www.sciencedirect.com/science/article/pii/0021929094900299

[56] P. Larson, "Comparison of foot strike patterns of barefoot and minimally shod runners in a recreational road race," *Journal of Sport and Health Science*, vol. 3, no. 2, pp. 137–142, Jun. 2014. [Online]. Available: https://www.sciencedirect.com/science/article/pii/S2095254614000283

[57] R. J. Full, T. Kubow, J. Schmitt, P. Holmes, and D. Koditschek, "Quantifying Dynamic Stability and Maneuverability in Legged Locomotion1," *Integrative and Comparative Biology*, vol. 42, no. 1, pp. 149–157, Feb. 2002. [Online]. Available: https://doi.org/10.1093/icb/42.1.149

[58] R. M. Magnani, S. M. Bruijn, J. H. van Dieën, and P. A. Forbes, "Stabilization demands of walking modulate the vestibular contributions to gait," *Scientific Reports*, vol. 11, p. 13736, Jul. 2021. [Online]. Available: https://www.ncbi.nlm.nih.gov/pmc/articles/PMC8253745/

[59] L. D'Hondt, D. Gupta, B. Van Den Bosch, T. J. W. Buurke, M. Afschrift, M. Febrer-Nafría, I. Vandekerckhove, and F. De Groote, "PREDSIM: A FRAMEWORK FOR RAPID PREDICTIVE SIMULATIONS OF LOCOMOTION," Kyoto, Jul. 2023.

[60] S. Delp, J. Loan, M. Hoy, F. Zajac, E. Topp, and J. Rosen, "An interactive graphics-based model of the lower extremity to study orthopaedic surgical procedures," *IEEE Transactions on Biomedical Engineering*, vol. 37, no. 8, pp. 757–767, Aug. 1990, conference Name: IEEE Transactions on Biomedical Engineering. [Online]. Available: https://ieeexplore.ieee.org/document/102791

[61] A. Rajagopal, C. L. Dembia, M. S. DeMers, D. D. Delp, J. L. Hicks, and S. L. Delp, "Full-Body Musculoskeletal Model for Muscle-Driven Simulation of Human Gait," *IEEE Transactions on Biomedical Engineering*, vol. 63, no. 10, pp. 2068–2079, Oct. 2016. [Online]. Available: http://ieeexplore.ieee.org/document/7505900/

[62] E. M. Arnold, S. R. Ward, R. L. Lieber, and S. L. Delp, "A Model of the Lower Limb for Analysis of Human Movement," *Annals of Biomedical Engineering*, vol. 38, no. 2, pp. 269–279, Feb. 2010. [Online]. Available: https://doi.org/10.1007/s10439-009-9852-5

[63] T. Geijtenbeek, "SCONE: Open Source Software for Predictive Simulation of Biological Motion," *Journal of Open Source Software*, vol. 4, no. 38, p. 1421, Jun. 2019. [Online]. Available: https://joss.theoj.org/papers/10.21105/joss.01421

[64] S. R. Hamner, A. Seth, and S. L. Delp, "Muscle contributions to propulsion and support during running," *Journal of Biomechanics*, vol. 43, no. 14, pp. 2709–2716, Oct. 2010. [Online]. Available: https://www.sciencedirect.com/science/article/pii/S0021929010003611

[65] N. Hansen, "The CMA Evolution Strategy: A Comparing Review," in *Towards a New Evolutionary Computation: Advances in the Estimation of Distribution Algorithms*, ser. Studies in Fuzziness and Soft Computing, J. A. Lozano, P. Larrañaga, I. Inza, and E. Bengoetxea, Eds. Berlin, Heidelberg: Springer, 2006, pp. 75–102. [Online]. Available: https://doi.org/10.1007/3-540-32494-1_4

[66] M. Millard, T. Uchida, A. Seth, and S. L. Delp, "Flexing Computational Muscle: Modeling and Simulation of Musculotendon Dynamics," *Journal of Biomechanical Engineering*, vol. 135, no. 021005, Feb. 2013. [Online]. Available: https://doi.org/10.1115/1.4023390

[67] T. Geijtenbeek, "The Hyfydy Simulation Software," Nov. 2021. [Online]. Available: https://hyfydy.com

[68] T. K. Uchida, J. L. Hicks, C. L. Dembia, and S. L. Delp, "Stretching Your Energetic Budget: How Tendon Compliance Affects the Metabolic Cost of Running," *PLOS ONE*, vol. 11, no. 3, p. e0150378, 2016, publisher: Public Library of Science. [Online]. Available: https://journals.plos.org/plosone/article?id=10.1371/journal.pone.0150378

[69] J. H. Wang, M. I. Iosifidis, and F. H. Fu, "Biomechanical basis for tendinopathy," *Clinical Orthopaedics and Related Research®*, vol. 443, pp. 320–332, 2006, publisher: LWW.

[70] R. Klemetti, P. Moilanen, J. Avela, and J. Timonen, "Effects of gait speed on stability of walking revealed by simulated response to tripping perturbation," *Gait & Posture*, vol. 39, no. 1, pp. 534–539, Jan. 2014. [Online]. Available: https://www.sciencedirect.com/science/article/pii/S0966636213006012

[71] S. R. Hamner and S. L. Delp, "Muscle contributions to fore-aft and vertical body mass center accelerations over a range of running speeds," *Journal of Biomechanics*, vol. 46, no. 4, pp. 780–787, Feb. 2013.

[72] A. A. Faisal, L. P. J. Selen, and D. M. Wolpert, "Noise in the nervous system," *Nature Reviews Neuroscience*, vol. 9, no. 4, pp. 292–303, Apr. 2008, number: 4 Publisher: Nature Publishing Group. [Online]. Available: https://www.nature.com/articles/nrn2258

[73] M. A. Busa, J. Lim, R. E. A. v. Emmerik, and J. Hamill, "Head and Tibial Acceleration as a Function of Stride Frequency and Visual Feedback during Running," *PLOS ONE*, vol. 11, no. 6, p. e0157297, Jun. 2016, publisher: Public Library of Science. [Online]. Available: https://journals.plos.org/plosone/article?id=10.1371/journal.pone.0157297

[74] J. A. García-Pérez, P. Pérez-Soriano, S. Llana Belloch, G. Lucas-Cuevas, and D. Sánchez-Zuriaga, "Effects of treadmill running and fatigue on impact acceleration in distance running," *Sports Biomechanics*, vol. 13, no. 3, pp. 259–266, Jul. 2014, publisher: Routledge _eprint: https://doi.org/10.1080/14763141.2014.909527. [Online]. Available: https://doi.org/10.1080/14763141.2014.909527

[75] C. Hall and C. J. Nester, "Sagittal Plane Compensations for Artificially Induced Limitation of the First Metatarsophalangeal Joint: A Preliminary Study," *Journal of the American Podiatric Medical Association*, vol. 94, no. 3, pp. 269–274, May 2004, publisher: The American Podiatric Medical Association Section: Journal of the American Podiatric Medical Association. [Online]. Available: https://japmaonline.org/view/journals/apms/94/3/0940269.xml

[76] O. Kramer, "Genetic Algorithms," in *Genetic Algorithm Essentials*, ser. Studies in Computational Intelligence, O. Kramer, Ed. Cham: Springer International Publishing, 2017, pp. 11–19. [Online]. Available: https://doi.org/10.1007/978-3-319-52156-5_2

[77] C. E. Bauby and A. D. Kuo, "Active control of lateral balance in human walking," *Journal of Biomechanics*, vol. 33, no. 11, pp. 1433–1440, Nov. 2000. [Online]. Available: https://www.sciencedirect.com/science/article/pii/S0021929000001019

[78] T. McGeer, "Passive Dynamic Walking," *The International Journal of Robotics Research*, vol. 9, no. 2, pp. 62–82, Apr. 1990, publisher: SAGE Publications Ltd STM. [Online]. Available: https://doi.org/10.1177/027836499000900206

[79] E. M. Arnold, S. R. Hamner, A. Seth, M. Millard, and S. L. Delp, "How muscle fiber lengths and velocities affect muscle force generation as humans walk and run at different speeds," *The Journal of Experimental Biology*, vol. 216, no. 11, pp. 2150–2160, Jun. 2013. [Online]. Available: https://www.ncbi.nlm.nih.gov/pmc/articles/PMC3656509/

[80] C. J. Dakin, J. T. Inglis, R. Chua, and J.-S. Blouin, "Muscle-specific modulation of vestibular reflexes with increased locomotor velocity and cadence," *Journal of Neurophysiology*, vol. 110, no. 1, pp. 86–94, Jul. 2013, publisher: American Physiological Society. [Online]. Available: https://journals.physiology.org/doi/full/10.1152/jn.00843.2012

[81] A. Prochazka, "Proprioceptive Feedback and Movement Regulation," in *Comprehensive Physiology*. John Wiley & Sons, Ltd, 2011, pp. 89–127, _eprint: https://onlinelibrary.wiley.com/doi/pdf/10.1002/cphy.cp120103. [Online]. Available: https://onlinelibrary.wiley.com/doi/abs/10.1002/cphy.cp120103

[82] P. K. Mutha, "Reflex Circuits and Their Modulation in Motor Control: A Historical Perspective and Current View," *Journal of the Indian Institute of Science*, vol. 97, no. 4, pp. 555–565, Dec. 2017. [Online]. Available: https://doi.org/10.1007/s41745-017-0052-2

[83] N. F. J. Waterval, K. Veerkamp, T. Geijtenbeek, J. Harlaar, F. Nollet, M. A. Brehm, and M. M. van der Krogt, "Validation of forward simulations to predict the effects of bilateral plantarflexor weakness on gait," *Gait & Posture*, vol. 87, pp. 33–42, Jun. 2021. [Online]. Available: https://www.sciencedirect.com/science/article/pii/S0966636221001417

[84] H. Geyer and H. Herr, "A Muscle-Reflex Model That Encodes Principles of Legged Mechanics Produces Human Walking Dynamics and Muscle Activities," *IEEE Transactions on Neural Systems and Rehabilitation Engineering*, vol. 18, no. 3, pp. 263–273, Jun. 2010, conference Name: IEEE Transactions on Neural Systems and Rehabilitation Engineering. [Online]. Available: https://ieeexplore.ieee.org/document/5445011

[85] S. Song and H. Geyer, "A neural circuitry that emphasizes spinal feedback generates diverse behaviours of human locomotion," *The Journal of Physiology*, vol. 593, no. 16, pp. 3493–3511, 2015, _eprint: https://onlinelibrary.wiley.com/doi/pdf/10.1113/JP270228. [Online]. Available: https://onlinelibrary.wiley.com/doi/abs/10.1113/JP270228

[86] J. Duysens, A. A. Tax, M. Trippel, and V. Dietz, "Increased amplitude of cutaneous reflexes during human running as compared to standing," *Brain Research*, vol. 613, no. 2, pp. 230–238, Jun. 1993.

[87] M. Edamura, J. Yang, and R. Stein, "Factors that determine the magnitude and time course of human H-reflexes in locomotion," *The Journal of Neuroscience*, vol. 11, no. 2, pp. 420–427, Feb. 1991. [Online]. Available: https://www.ncbi.nlm.nih.gov/pmc/articles/PMC6575227/

[88] G. Courtine, S. J. Harkema, C. J. Dy, Y. P. Gerasimenko, and P. Dyhre-Poulsen, "Modulation of multisegmental monosynaptic responses in a variety of leg muscles during walking and running in humans," *The Journal of Physiology*, vol. 582, no. 3, pp. 1125–1139, 2007, _eprint: https://onlinelibrary.wiley.com/doi/pdf/10.1113/jphysiol.2007.128447. [Online]. Available: https://onlinelibrary.wiley.com/doi/abs/10.1113/jphysiol.2007.128447

[89] T. C. Pataky, M. A. Robinson, and J. Vanrenterghem, "Vector field statistical analysis of kinematic and force trajectories," *Journal of Biomechanics*, vol. 46, no. 14, pp. 2394–2401, Sep. 2013. [Online]. Available: https://www.sciencedirect.com/science/article/pii/S0021929013003564

[90] "One-dimensional statistical parametric mapping in Python," iSSN: 1025-5842. [Online]. Available: https://www.tandfonline.com/doi/epdf/10.1080/10255842.2010.527837?needAccess=true&role=button

A Controllers

An overview of which feedback pathways are present and which parameters are optimized is shown in table 1.

		Walking model			Running model
Muscle	Reflex type	Stance	Lift-off	Swing	
Glut. max.	Mono		C0	KF	KL KF C0
	Ant.				KL KF
	Vest.	KP KV P0 C0			
Iliacus	Mono		C0	KL L0	KL KF C0
	Ant.			KL L0 (hamstrings)	KL KF
	Vest.	KP KV P0 C0		KP KV P0	
Psoas	Mono		C0	KL L0	KL KF C0
	Ant.				KL KF
	Vest.	KP KV P0		KP KV P0	
Hamstring	Mono			KF	KL KF C0
	Ant.				KL KF
	Vest.	KP KV P0 C0			
Rect. Fem.	Mono	KL L0 KF	KL L0 KF	KL L0 KF	KL KF C0
	Ant.				KL KF
	Vest.	KP KV P0 C0			
BiFem. SH.	Mono	KL L0 KF	KL L0 KF	KL L0 KF	KL KF C0
	Ant.				KL KF
	Vest.				
Vasti	Mono	KF C0*			KL KF C0
	Ant.				KL KF
	Vest.				
Gastroc.	Mono	KF	KF		KL KF C0
	Ant.				KL KF
	Vest.				
Soleus	Mono	KF	KF		KL KF C0
	Ant.				KL KF
	Vest.				
Tib. Ant	Mono	KL L0	KL L0	KL L0	KL KF C0
	Ant.	KF (soleus)	KF (soleus)	KF (soleus)	KL KF
	Vest.				

* is a conditional reflex based on the position of the knee

Table 1: An overview of the reflexgains that were implemented in the controllers of both models. Reflexes were grouped in mono and antagonistic muscle reflexes and vestibular reflexes. For the muscle reflexes: KL and KF are the respective length and force feedback gains. C0 is a constant. L0 is a constant that is subtracted from the muscle length. For the vestibular reflexes: KP and KV are the respective position and velocity feedback gains. C0 is a constant. P0 is subtracted from the muscle length. P0 is only optimized if no C0 is present. The source muscle is given for the antagonistic reflexes.

B Baseline performance Statistical tests

To compare the simulations from this study results with the experimental data from Hamner and Delp [71] statistical parametric mapping (SPM) was used, following the method that is described in Pataky et al. [89]. The main advantage of using SPM is the possibility of comparing trajectory data, removing the need to rewrite one dimensional data, such as joint angles over time, to zero dimensional data such as the peak joint angles. This would result in a loss of data. Furthermore, an SPM analysis allows for non-directed hypotheses. One does not have to know on forehand were the differences are expected. This results in a broader and thus more complete comparison between to data sets. In SPM, the trajectories of multiple variable are compared, resulting in a one dimensional data set of where the trajectories differ significantly. The results of the predicted motion of the base model were tested against the experimental data using a two-tailed t-test. The tests were executed using the SPM1D python package. [90]

Using these tests it was shown that the largest discrepancies in kinematics were indeed found during the stancphase (see figure 11).

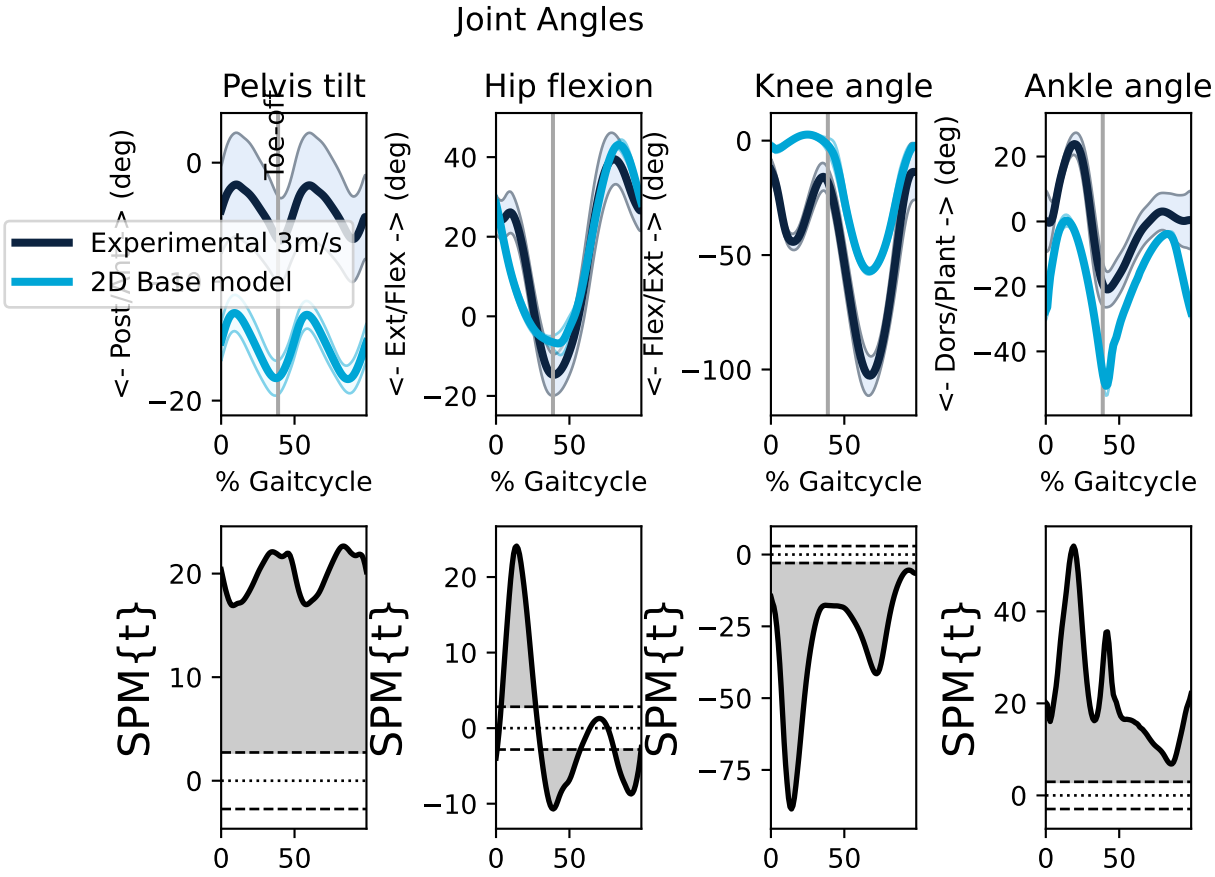

Figure 11: Kinematics of the 2D running model compared to the experimental data. The biggest differences are found during stance phase. The plots in the second row show the statistical differences between the experimental data and the running model outcomes. The larger the SPMt value, the larger the differences. All areas that are marked grey are significantly different ($p<0.001$)

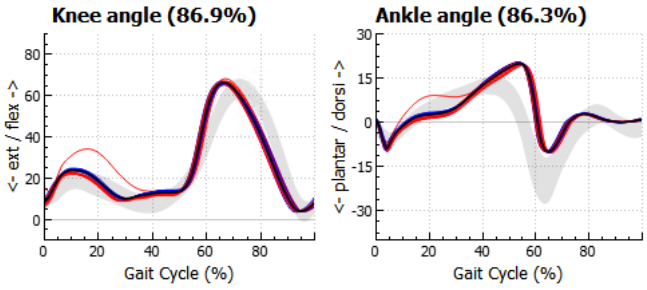

Figure 12: Kinematics of the 2D walking model compared to the experimental data. The grey shaded area is the experimental data.

C Maximum isometric forces

S_MSK5 did not come to a stable gait pattern because it did not have enough muscle force to get to a running gait pattern. This is confirmed by the muscle activation patterns (Figure 14, which show multiple muscles coming to maximum activation, while the forward speed is not 3m/s.

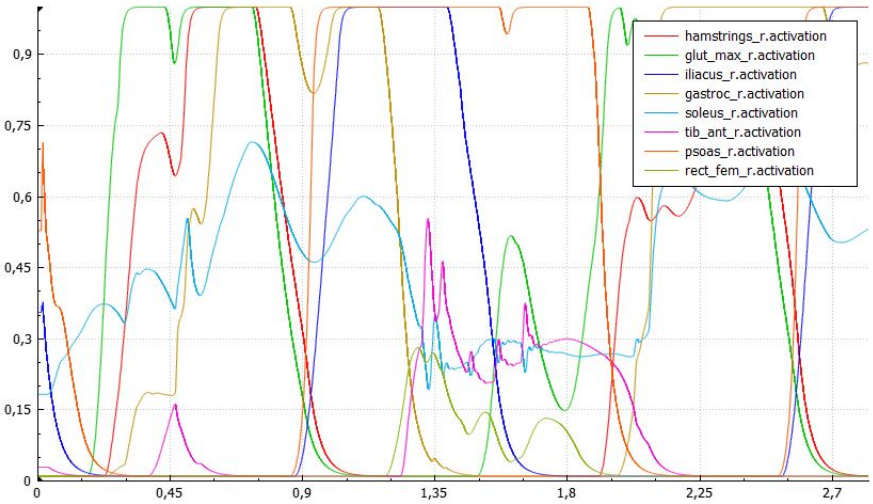

Figure 13: The activations of all rightsided muscles in S_MSK5.

D S_H1120_WALK + RUN

Implementing the musculoskeletal model or the objective function of H0920_RUN in H1120_WALK does not decrease the realism of the simulations.

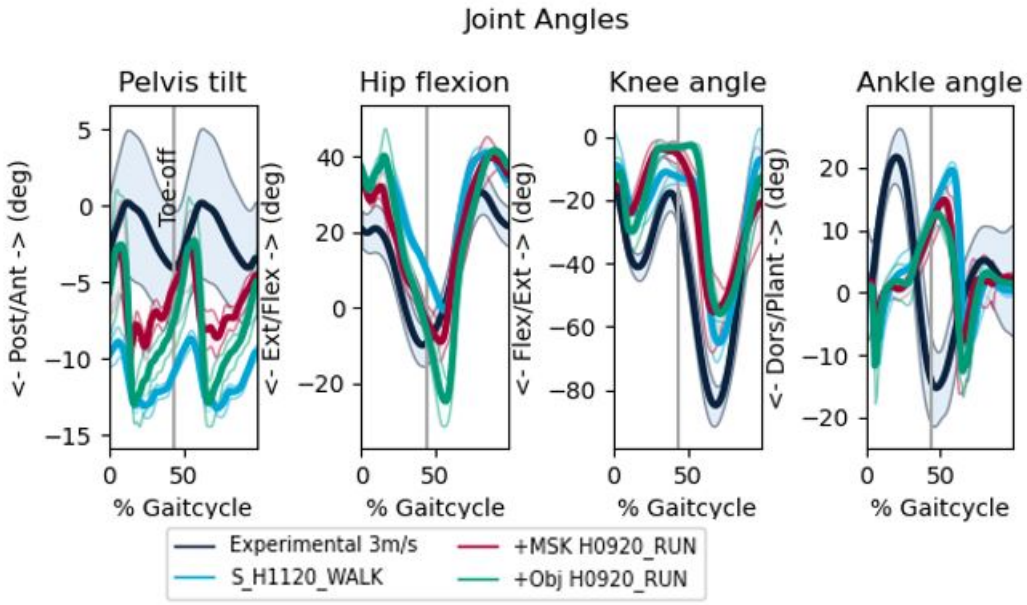

Figure 14: Kinematics of S_H1120_WALK with different components of H0920_RUN implemented

E Additional plots biomechanics

In this appendix, the supporting figures are given for the hypotheses that were tested in this study. A complete overview of these hypotheses is shown in figure 9

E.1 Controller

E.1.1 Feedback pathways

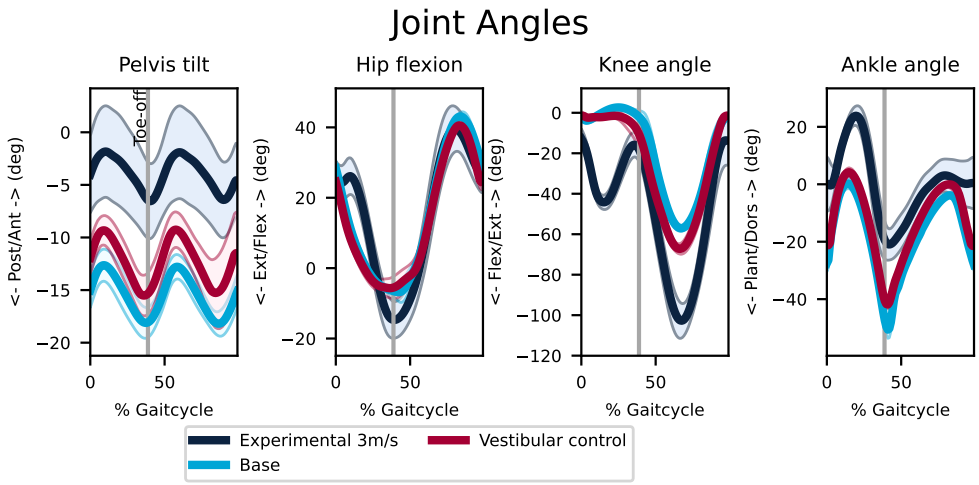

Figure 15: Joint Angles for a scenario with and without vestibular control

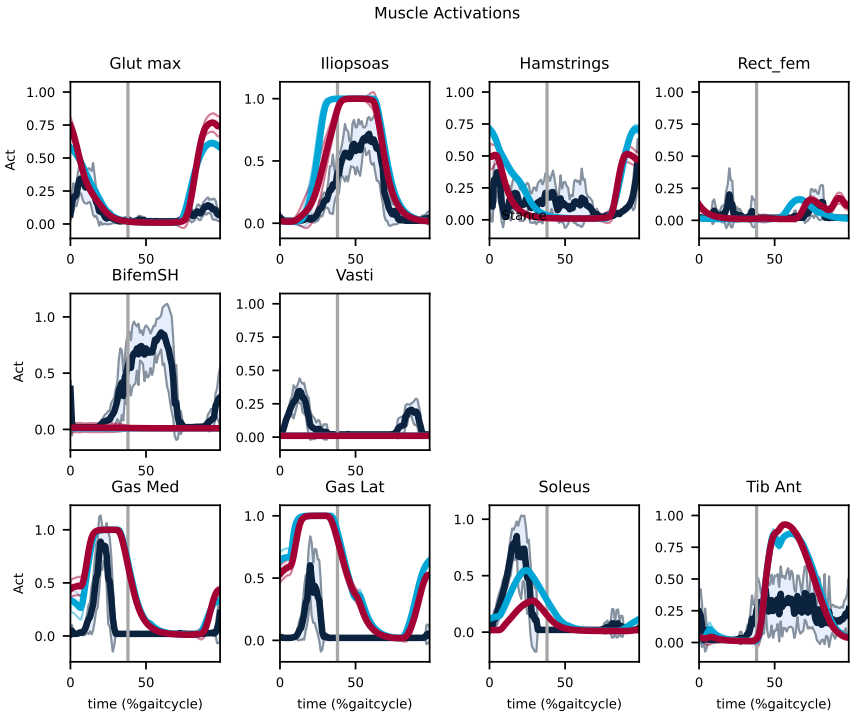

Figure 16: Muscle activation for a scenario with and without vestibular control

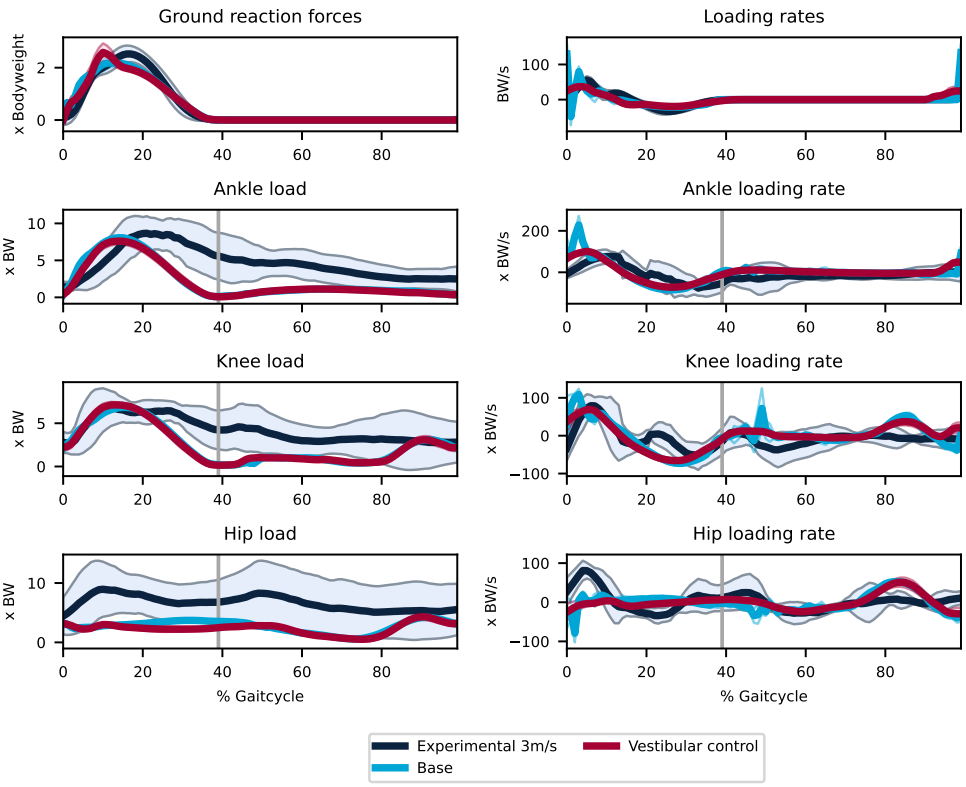

Figure 17: Ground reaction forces, joint loads and their respective rates for a scenario with and without vestibular control

E.1.2 Stability

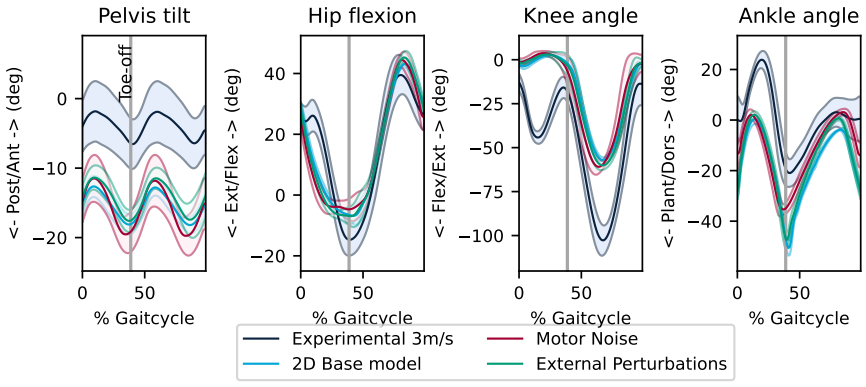

Figure 18: Joint Angles for different stability scenarios

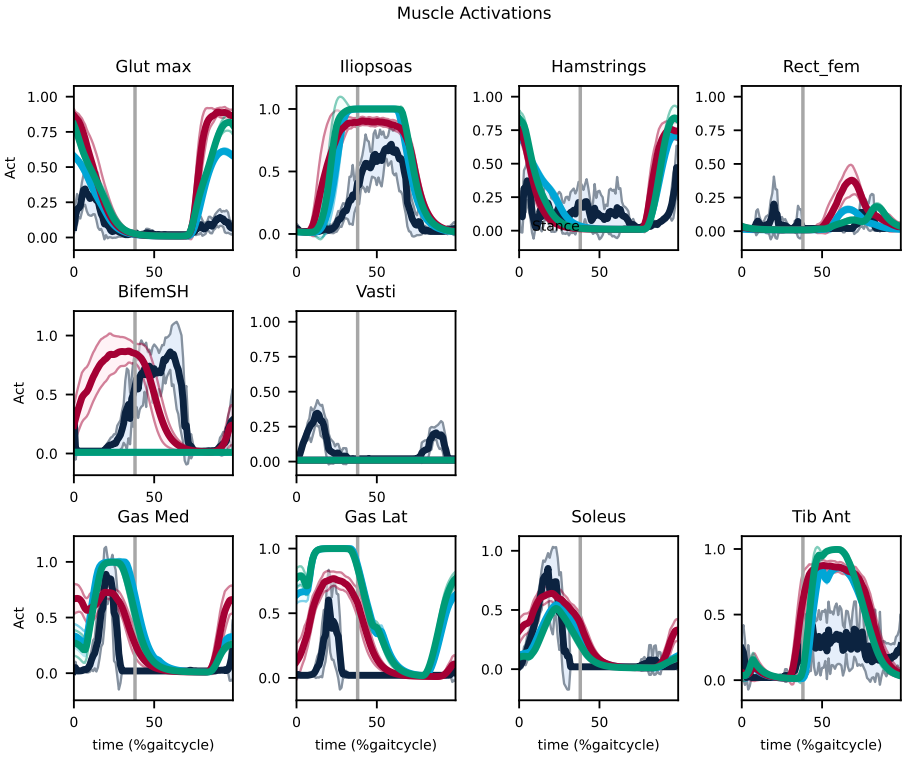

Figure 19: Muscle activation for different stability scenarios

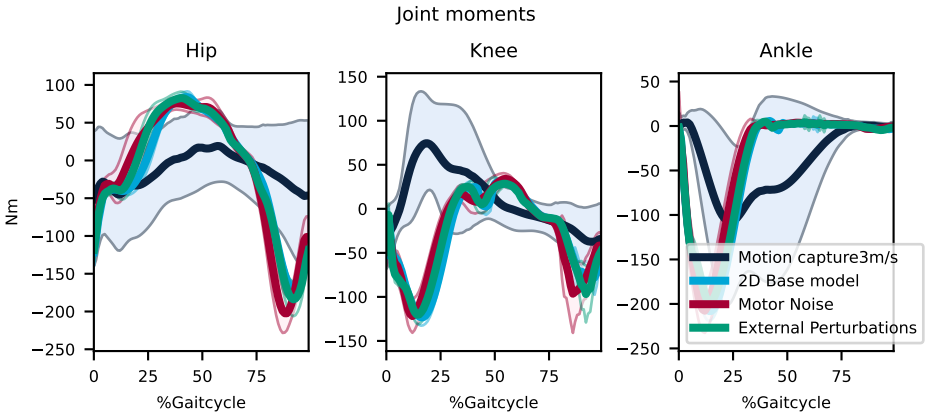

Figure 20: Joint moments for different stability scenarios

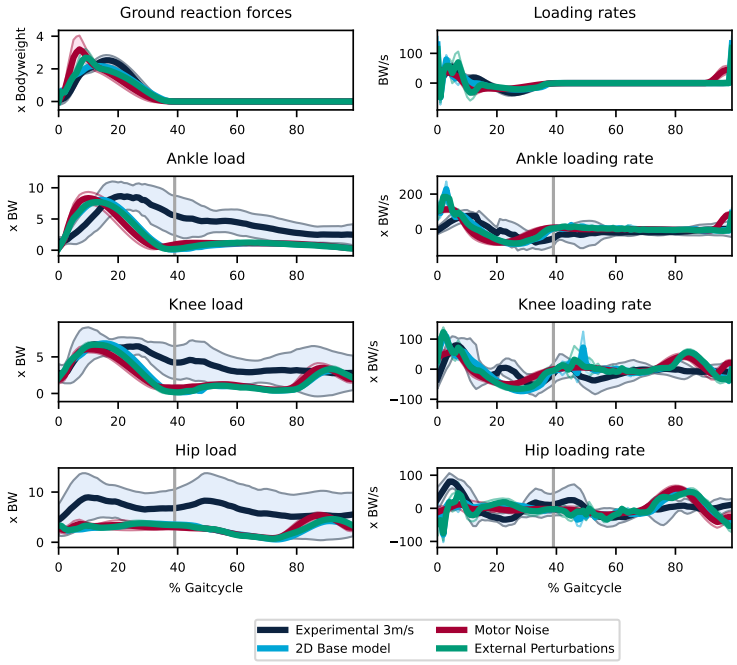

Figure 21: Ground reaction forces, joint loads and their respective rates for different stability scenarios

E.2 MSK model

E.2.1 Walking model

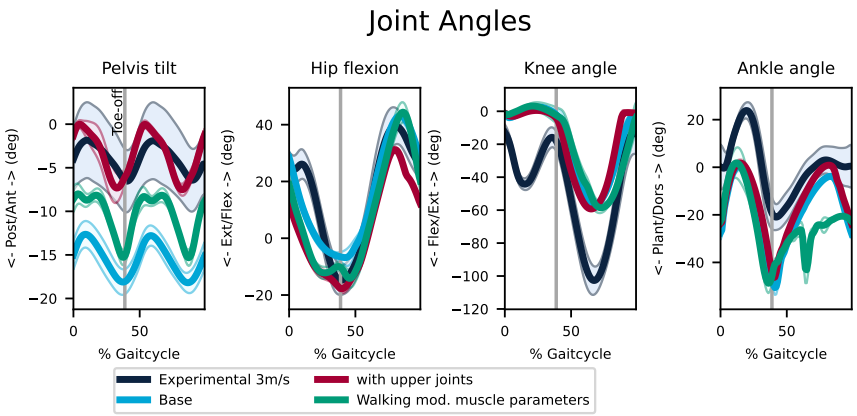

Figure 22: Joint Angles for different MSK alterations based on the walking model

E.3 Implementations in the walking model

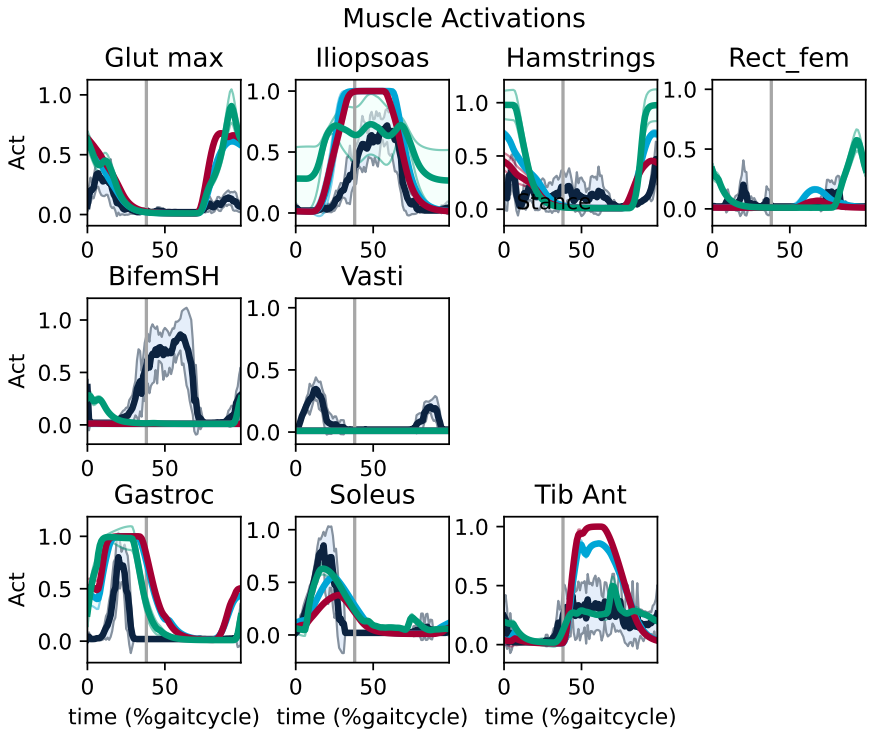

Figure 23: Muscle activation for different MSK alterations based on the walking model

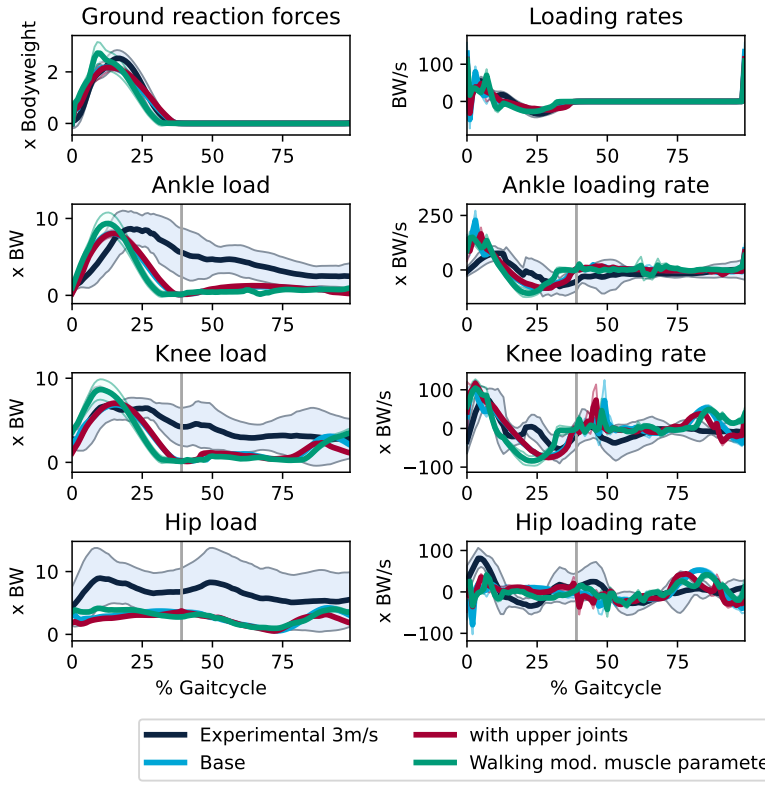

Figure 24: Ground reaction forces, joint loads and their respective rates for different MSK alterations based on the walking model

E.4 Foot Contact model

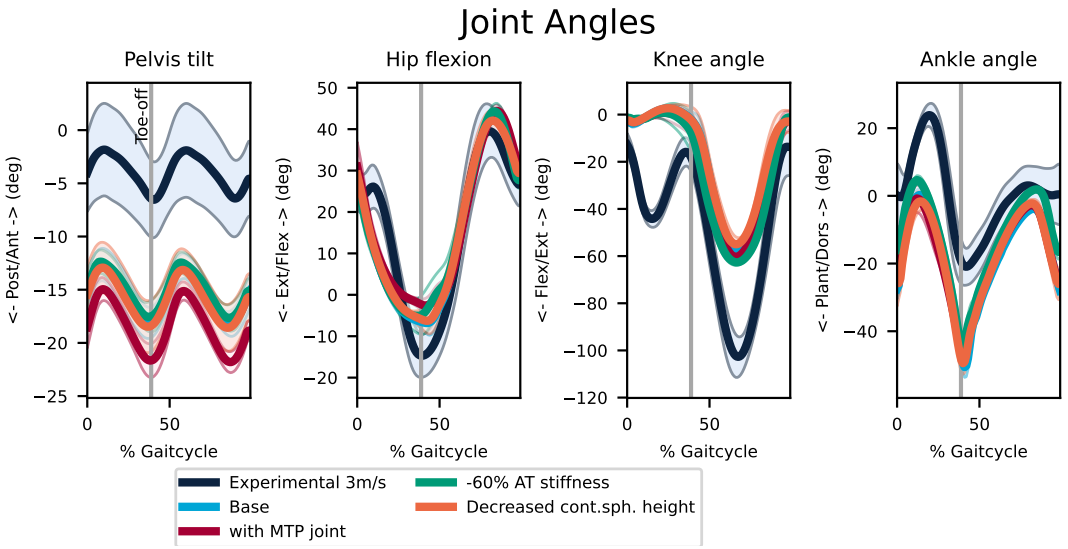

Figure 25: Joint Angles for different proposed solutions by Falisse et al. [47]

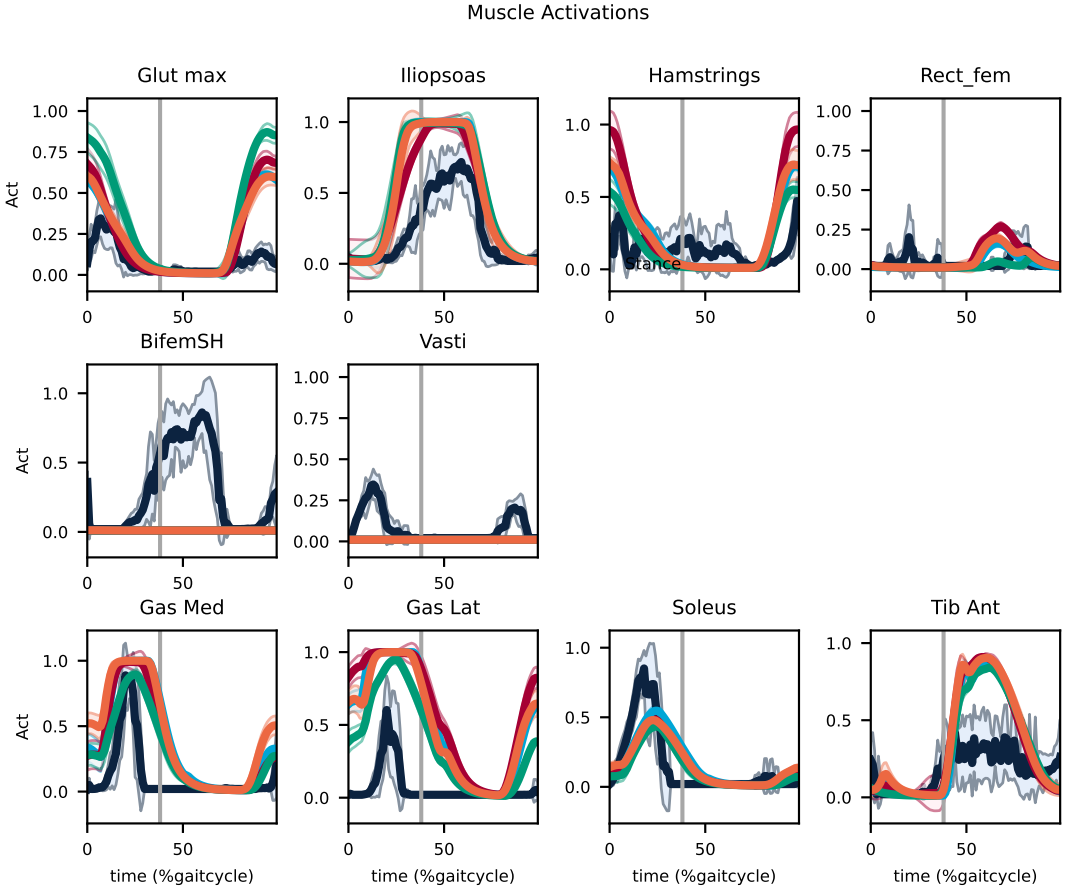

Figure 26: Muscle activation for different proposed solutions by Falisse et al. [47]

E.5 Objective

E.5.1 main

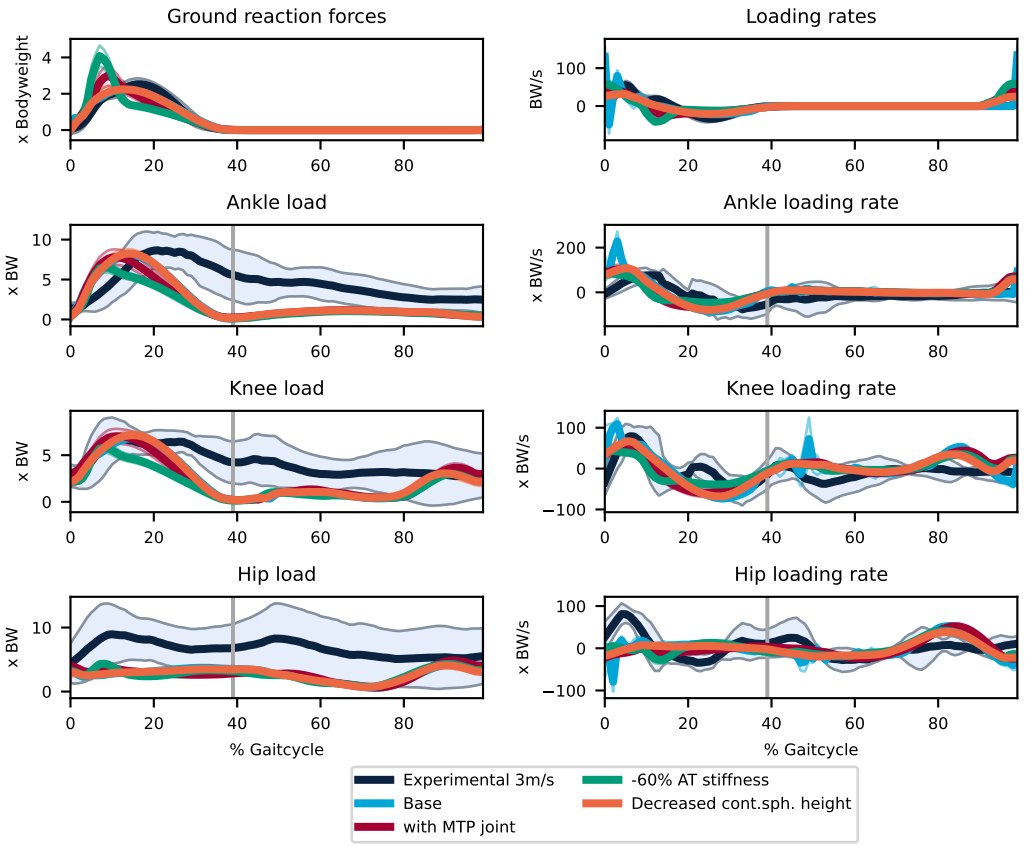

Figure 27: Ground reaction forces, joint loads and their respective rates for different proposed solutions by Falisse et al. [47]

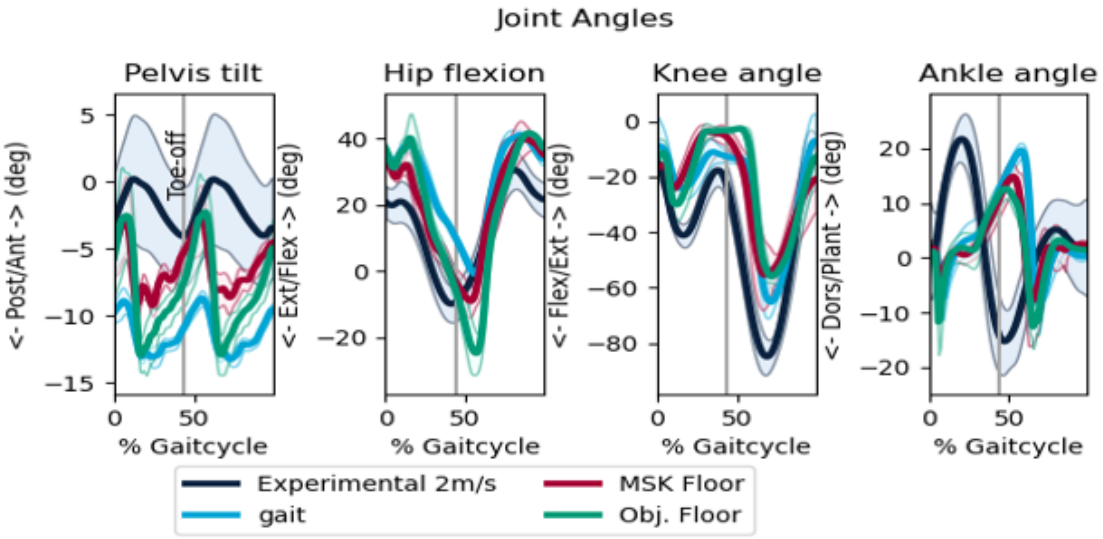

Figure 28: Effects of adapting MSK or objective in walking model

E.5.2 Penalty

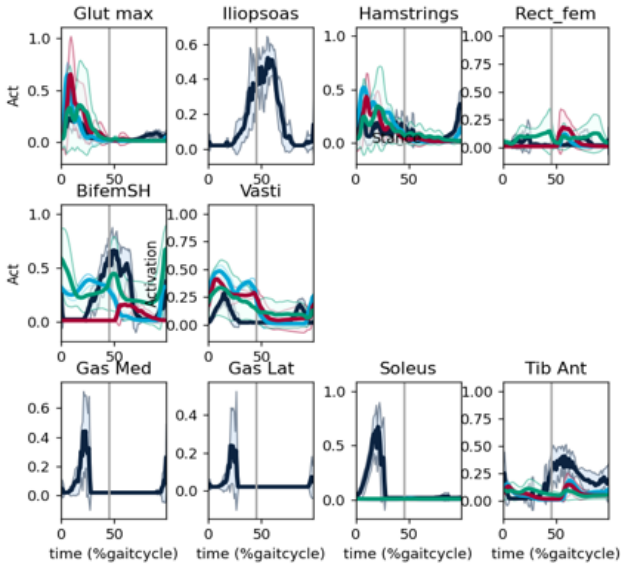

Figure 29: Effects of adapting MSK or objective in walking model

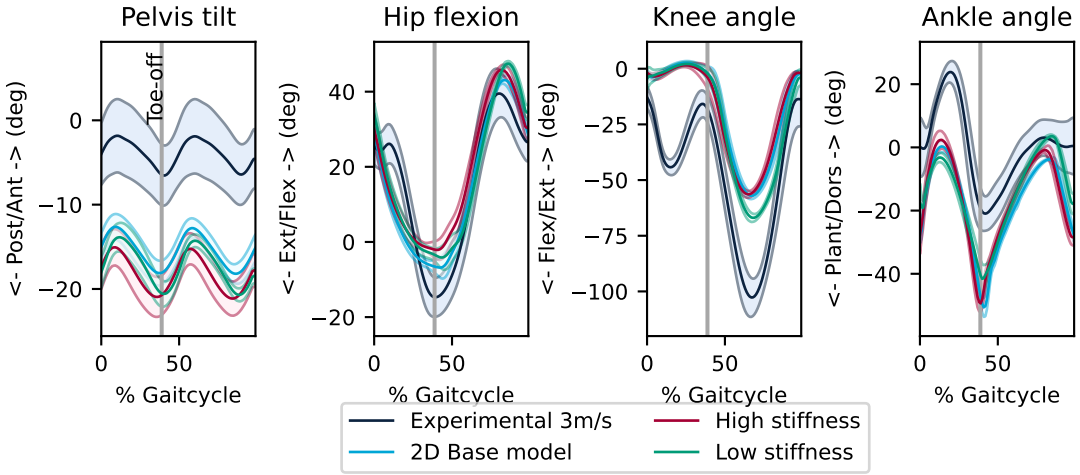

Figure 30: Joint Angles for different contact sphere stiffness scenarios

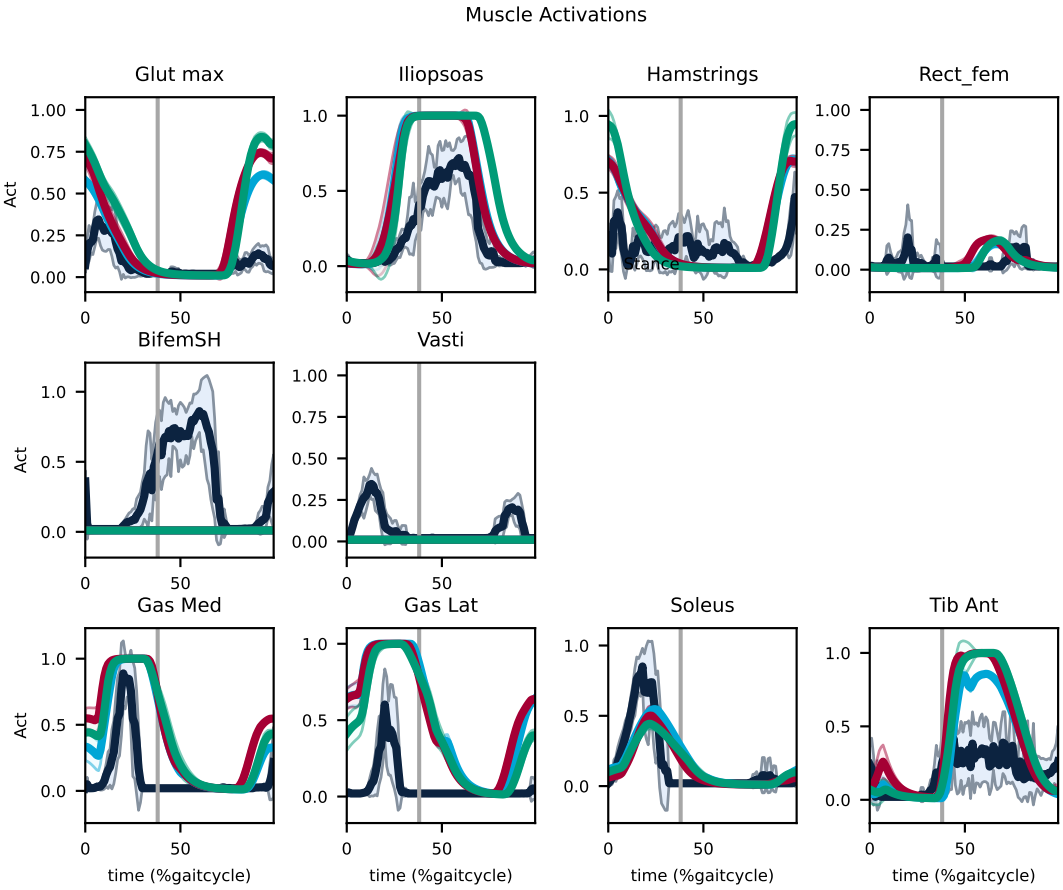

Figure 31: Muscle activation for different contact sphere stiffness scenarios

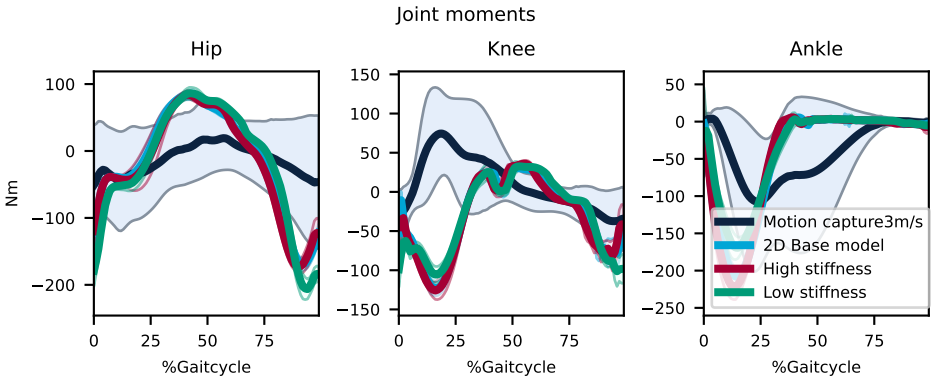

Figure 32: Joint moments for different contact sphere stiffness scenarios

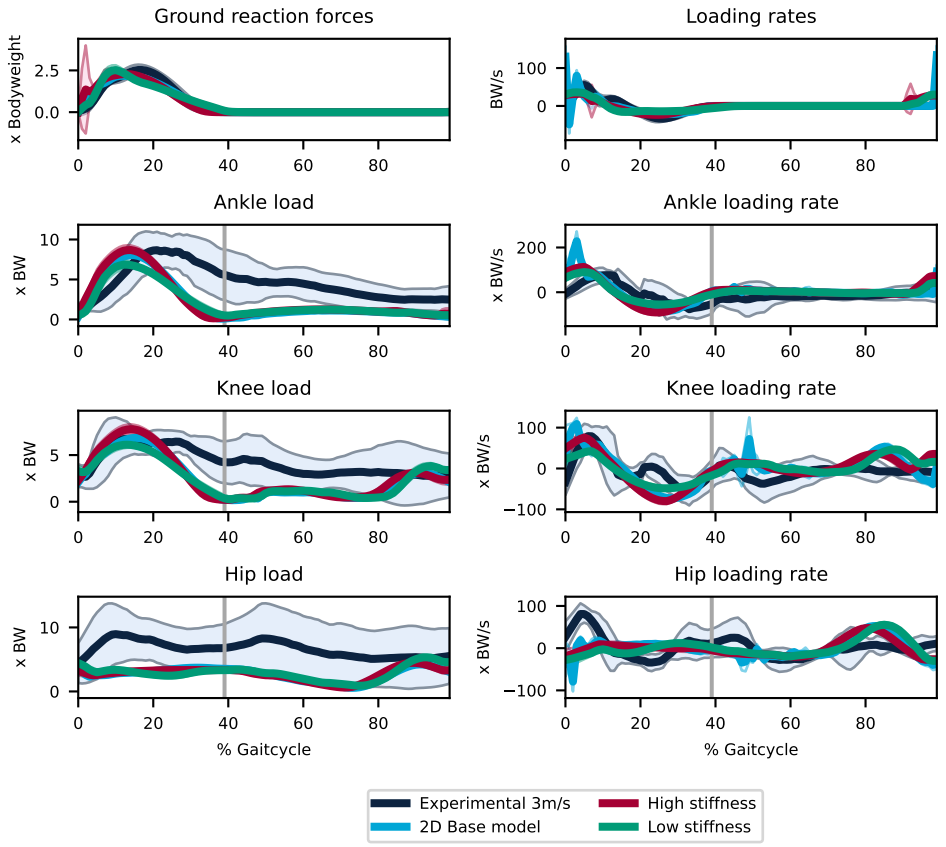

Figure 33: Ground reaction forces, joint loads and their respective rates for different contact sphere stiffness scenarios

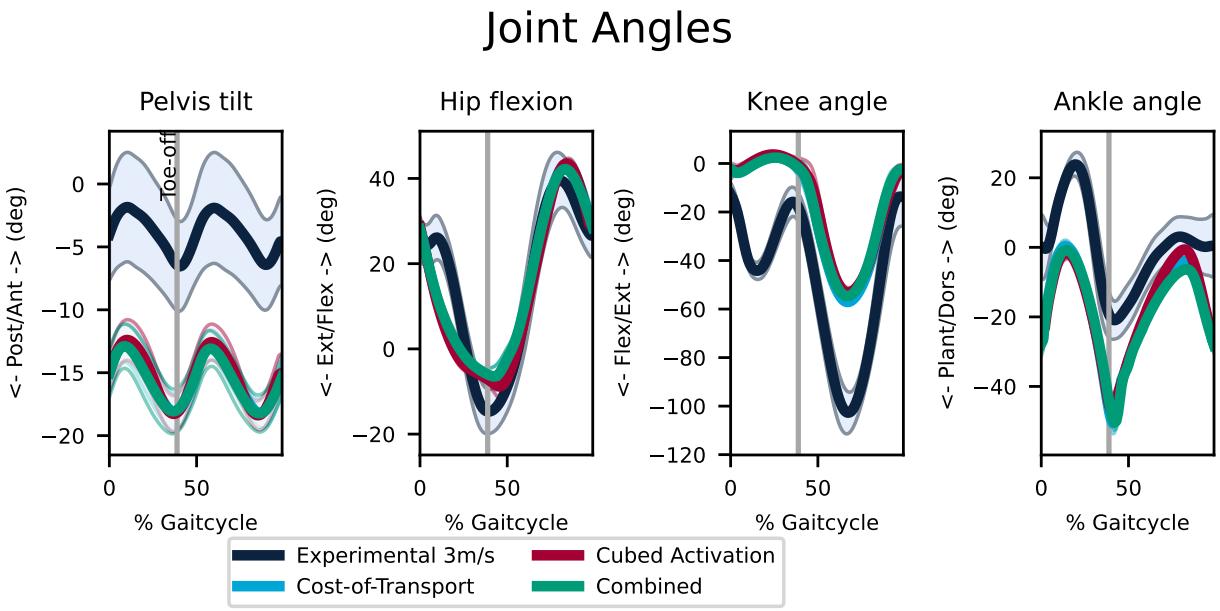

Figure 34: Joint Angles for different objectives

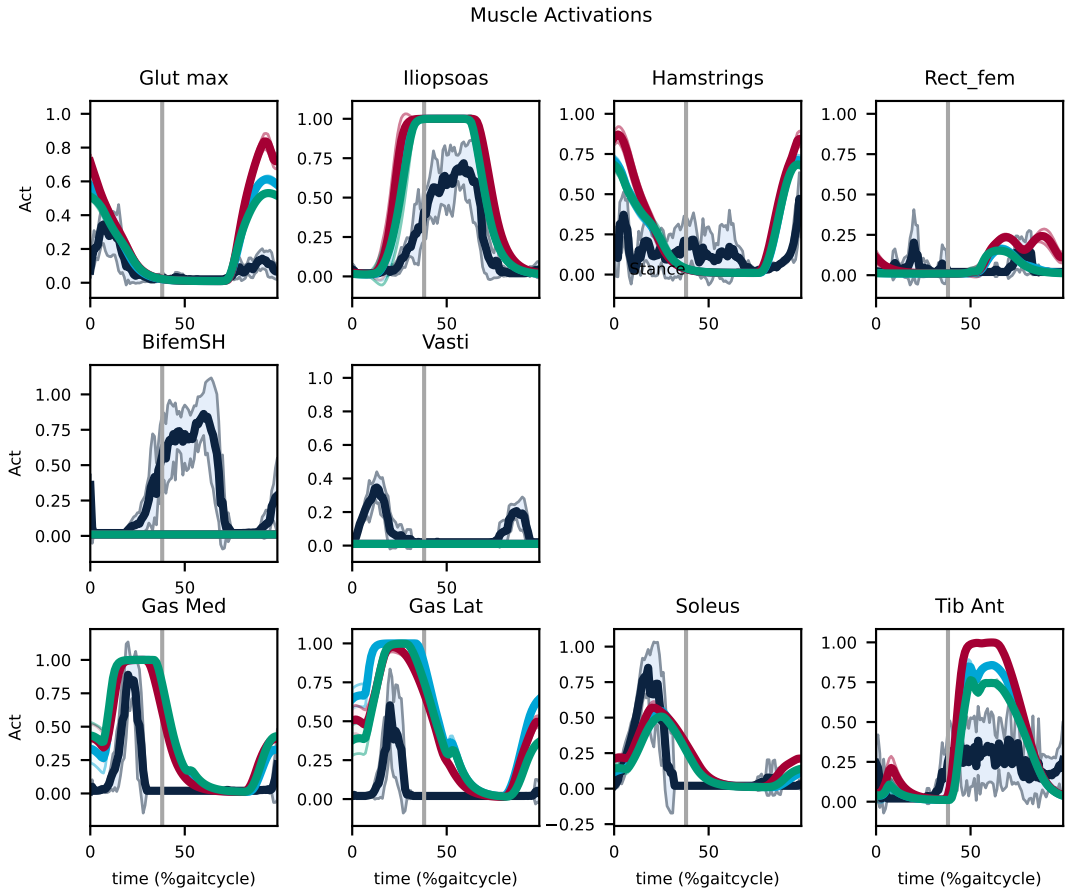

Figure 35: Muscle activation for different objectives

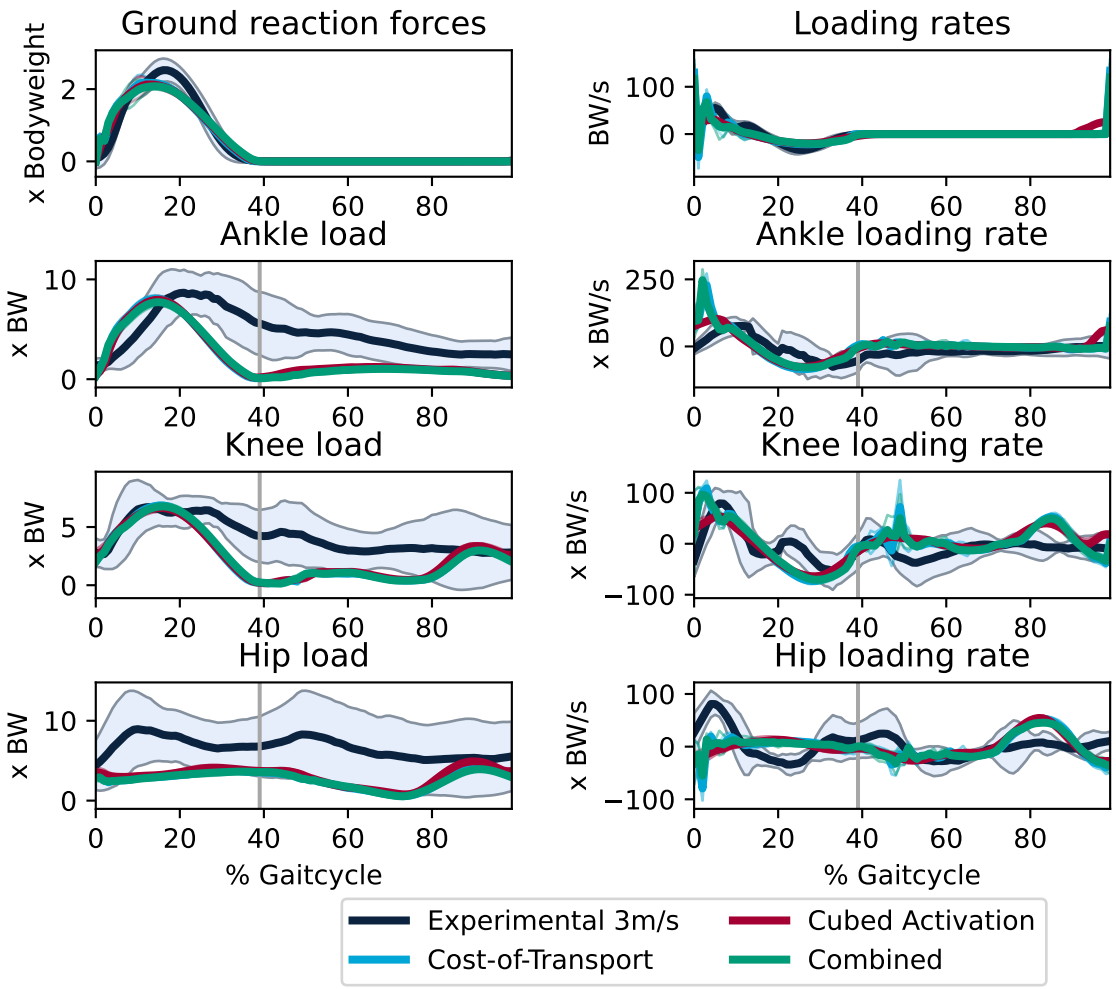

Figure 36: Ground reaction forces, joint loads and their respective rates for different objectives

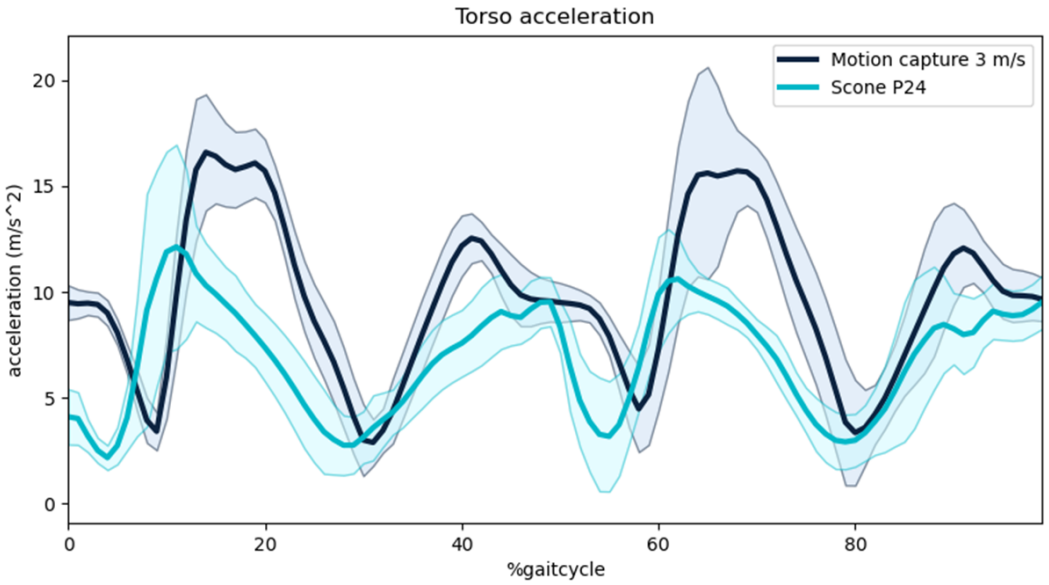

Figure 37: The torsional acceleration of the base running model compared to the experimental data

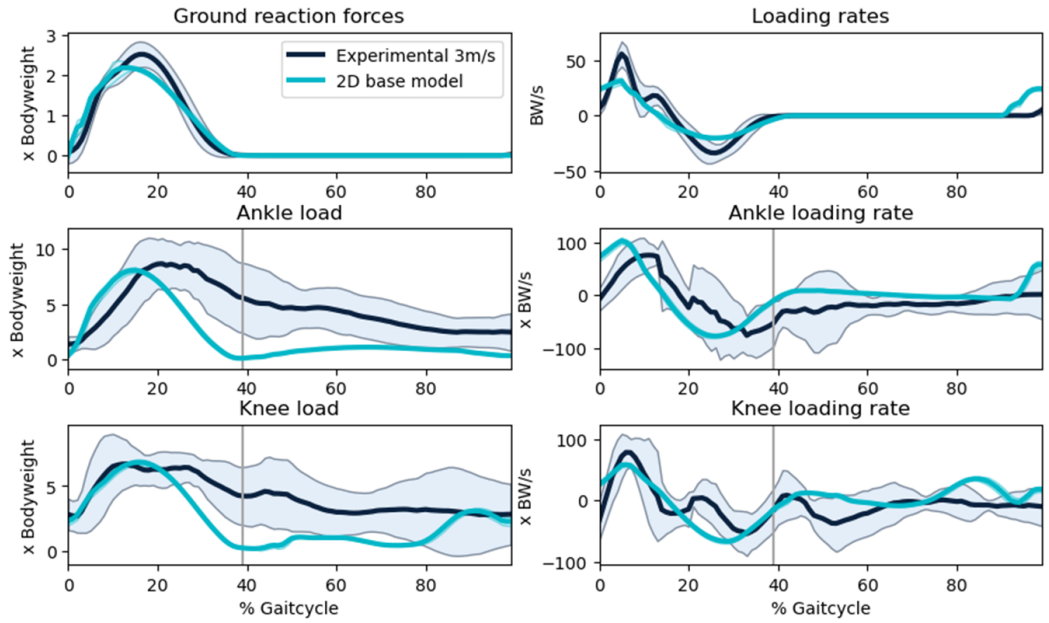

Figure 38: Ground reaction forces and joint loads of the baseline running model,compared to the experimental data

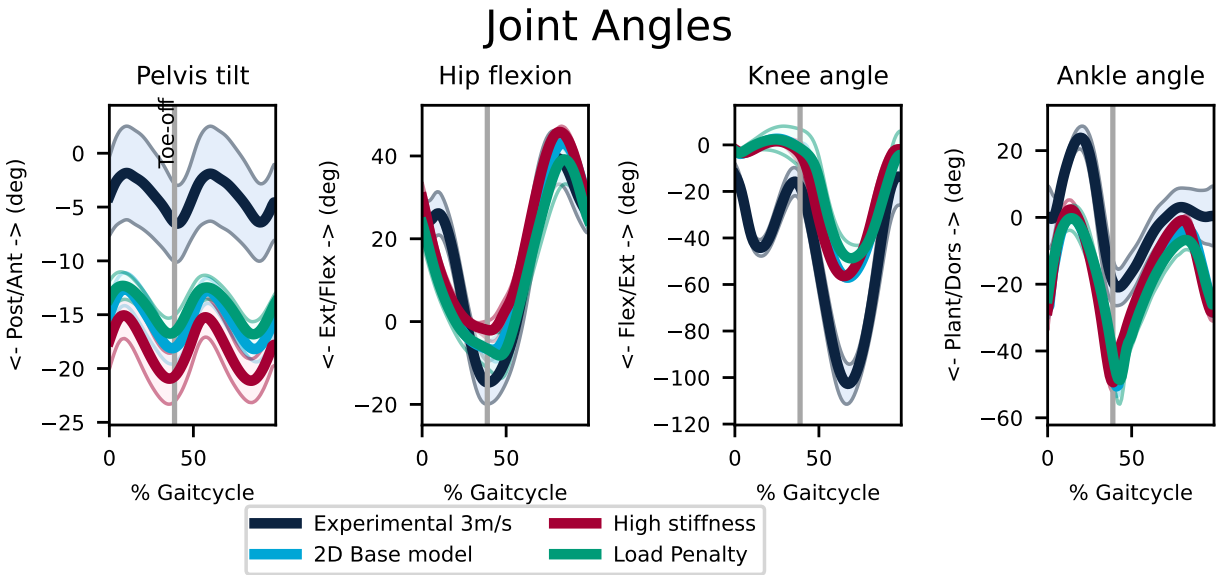

Figure 39: Joint Angles for a high contact stiffness and joint load penalty scenario

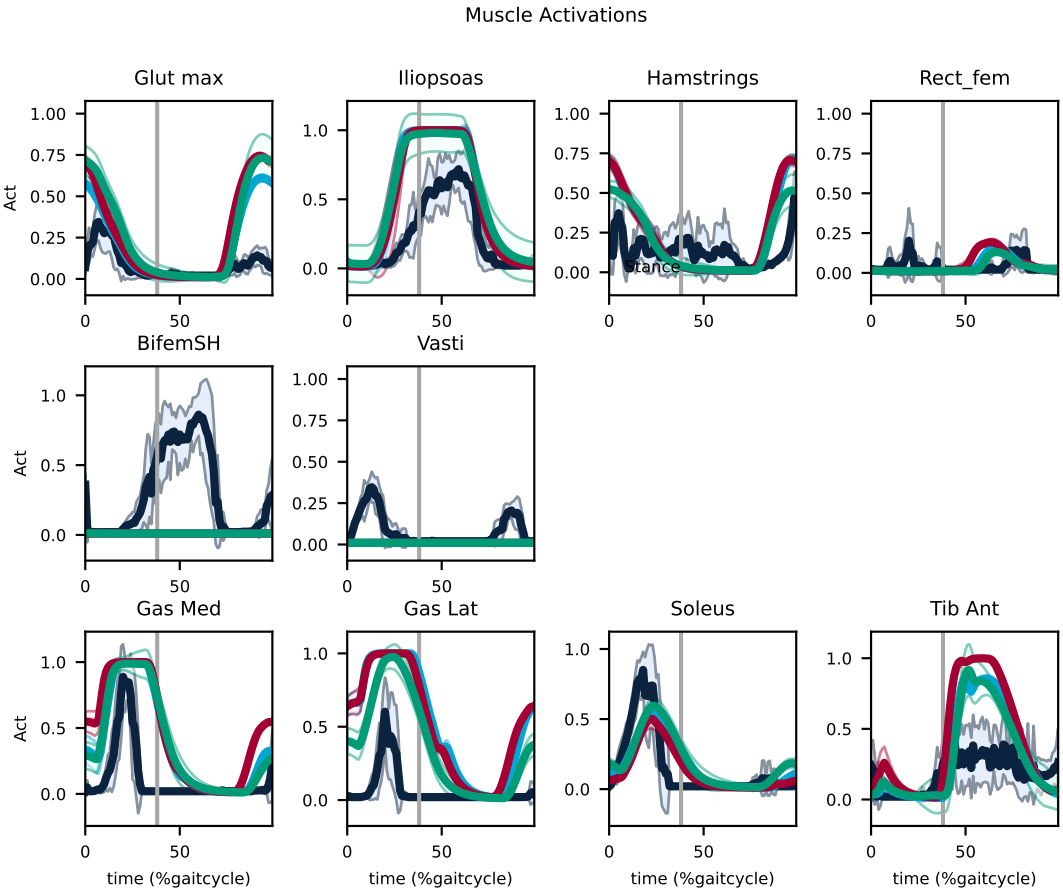

Figure 40: Muscle activation for a high contact stiffness and joint load penalty scenario

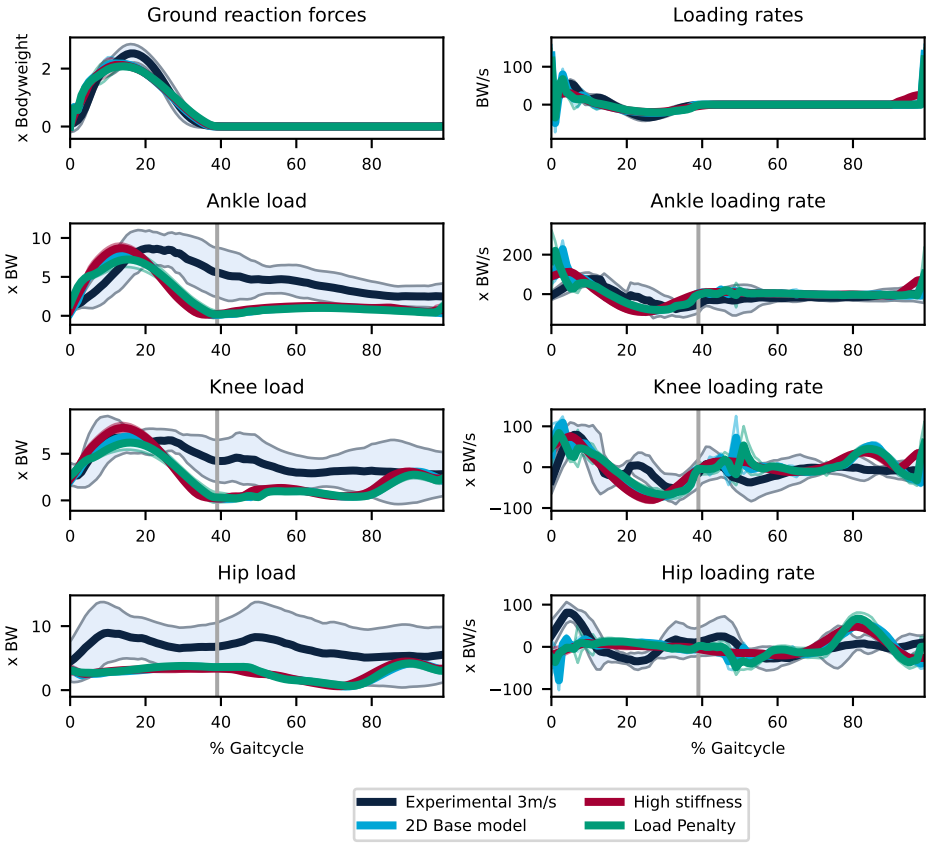

Figure 41: Ground reaction forces, joint loads and their respective rates for a high contact stiffness and joint load penalty scenario